AN ABSTRACT OF THE THESIS OF

Axel Destremau for the degree of Master of Science in Mechanical Enginering, presented November 7, 1991.

Title: Natural Convection Cooling of Vertical Plates in an Enclosure — A Numerical Simulation

Redacted for Privacy

Abstract approved: James R. Welty

The cooling of three plates within an enclosure was numerically simulated. The plates were uniformly heated and the enclosure kept at constant temperature. The simulation was performed using TEMPEST, a code which solves the Navier Stokes equations and the energy equation.

The middle plate remained stationary while the two other plates were moved symmetrically away from the middle line. The distance, b, separating the middle plate from the other plates was allowed to vary while other parameters were kept at constant values. Temperature, velocity, and the Nusselt number were computed as was the corresponding channel Rayleigh number. Streamline and isotherm plots were constructed.

The significant results of this study are the following:

1) The average Nusselt number correlates with the channel Rayleigh number as

$$Nu = \left((0.131 Ra^{0.5})^{-6} + (0.278\ Ra^{0.2})^{-6} \right)^{-1/6}$$

2) The optimum position for the intermediate vertical plate was found for three different heat flux levels. At the lowest value of heat flux, 10^3 W/m^3, there was one location (b_{opt}) where the plate temperature was a minimum. At the other heat flux levels examined (10^4 W/m^3, 10^5 W/m^3) there was a range for b_{opt} where the plate temperature experienced a minimum value. These optima are

- $b_{opt} = 0.021$ m for $q''' = 10^4$ W/m^3
- $b_{opt} \begin{cases} > 0.009 \text{ m} \\ < 0.030 \text{ m} \end{cases}$ for $q''' = 10^4$ W/m^3
- $b_{opt} \begin{cases} > 0.010 \text{ m} \\ < 0.030 \text{ m} \end{cases}$ for $q''' = 10^5$ W/m^3

Natural Convection Cooling of Vertical Plates in an Enclosure — A Numerical Simulation

by

Axel Destremau

A THESIS

Submitted to

Oregon State University

in partial fulfillment of

the requirements for the

degree of

Master of Science

Completed December 13, 1991

Commencement June 1992

APPROVED

Redacted for Privacy

Professor of Mechanical Engineering in charge of major

Redacted for Privacy

Head Department of Mechanical Engineering

Redacted for Privacy

Dean of Graduate School

Date thesis is presented December 13, 1991

Typed by Axel DESTREMAU

ACKNOWLEDGMENTS

I would like to thank very much my major professor, Dr. James R. Welty, for his constant encouragements and for giving me some of his very precious time.

In addition, I would like to address my thanks to Dr. Donald Trent without the help of whom this project would have taken me a much longer time.

Also, I would like to thank my office mates, Sean Kopczynski and Doug Snell for bearing my presence in the same office and sharing various thoughts.

Finally, I want to dedicate this work to my father, Thierry Destremau, who made this two years in the United State possible.

TABLE OF CONTENTS

LIST OF FIGURES

NOMENCLATURE

A	Constant in the Churchill and Usagi correlation procedure
a	Plate width
B	Constant in the Churchill and Usagi correlation procedure
b	Channel width
g	Gravitational constant
Gr	Grashoff number
H	Height of the enclosure
L	Width of the total enclosure
L_1	Distance from the wall to the plate A
L_2	Distance from the bottom wall to the bottom of the plates
L_3	Height of the channel
n	Exponent to find in the Churchill and Usagi method
Nu	Average Nusselt number
P	Non-dimensional pressurein the enclosure
p	Pressure in the enclosure
Pr	Prantl number
Q	Total heat dissipated by the plates
$\overline{q''}$	Average heat flux in the channel
q"	Heat flux

q_1	Heat flux on the channel side of plate A
q_2	Heat flux on the channel
R	Channel aspect ratio L_3/b
Ra"	Average Rayleigh number
r_h	Heat flux ratio
r_t	Temperature ratio
T	Non-dimensional temperature
t	Temperature
$\bar{t}$	Average temperature
T_1	Non-dimensional temperature on plate A
$t_{1,1/2}$	Temperature at midheight on plate A
$T_{1/2}$	Non-dimensional temperature at midheight on plate A
T_2	Non-dimensional temperature on plate B
$t_{2,1/2}$	Temperature at midheight on plate B
T_o	Non-dimensional reference temperature
t_o	Reference temperature
U	Non-dimensional X-component velocity
u	x-component velocity
V	Non-dimensional Y-component velocity
v	y-component velocity
X	Non-dimensional Cartesian coordinate
x	Cartesian coordinate
Y	Non-dimensional Cartesian coordinate
y	Cartesian coordinate

Greek symbol

ν	Kinematic viscosity of fluid
ρ	Density of fluid
α	Thermal diffusivity
ψ	Stream function
β	Coefficient of thermal expansion of fluid
Γ	Channel aspect ratio

Subscript

1	Right face of plate A
2	Left face of plate B
i,j	Index for finite difference
opt	optimum value
max	maximum

Natural Convection Cooling of Vertical Plates in an Enclosure - A Numerical Simulation

Chapter I: Introduction

Natural convection cooling by air has many applications in different industries, but it is of particular interest in the electronic industry. The main application is the cooling of Printed Circuit Boards (PCB). As in any array of PCB, heat dissipating components are mounted to a plate and heat transfer from the array to the surroundings is influenced by natural convection and radiation as well as by conduction in the plates. Many applications can be approximated with little error as smooth plates with isothermal or uniform flux surfaces. Although forced convection is the most widely used heat transfer mode, natural convection cooling is important since it is the least expensive, quietest and most reliable method of heat rejection. Natural convection cooling of open channels has been studied extensively and many correlations are available. However, very little work has been done for channels in an enclosure.

In this paper, a three-plate array in an enclosure, kept at constant temperature, has been studied numerically. The plates were heated with a uniform heat source. The middle plate, referred to as plate B, was fixed in the middle of the enclosure. The two remaining plates were moved, symmetrically, to change the channel aspect ratio,

as shown in Figure 1. Due to symmetry, only the left plate, referred to as plate A, was used in the numerical simulation. The space between plate A and B will be referred to as the channel. Radiation heat transfer from the plates and conduction heat transfer in the plates were not considered in this study.

For short channels or/and large spacings between the plates, independent boundary layer development occurs at each surface and conditions correspond to those for a single plate. For large channel aspect ratios, L_3/b, developing boundary layers on opposing faces will eventually merge to form a fully-developed condition.

Different configurations were simulated to arrive at a correlation for the average Nusselt number, using the method of Churchill and Usagi [13]. In addition, the optimum spacing value for best cooling was determined. Comparative descriptions of the flow and the temperature in the enclosure are also included in this study. A comparison of results obtained from these simulations with those from the literature is presented. This comparison validates the results obtained.

CHAPTER II: LITERATURE REVIEW

The first paper written on the subject of cooling of vertical plates by natural convection, which remains as a major source of information, was written in 1942 by Elenbaas [1]. He studied the phenomenon of heat dissipation from parallel vertical plates by free convection and developed the following correlation for the Nusselt number:

$$Nu = \frac{1}{24} Ra''\left(1-\exp\left(\frac{-35}{Ra''}\right)\right)^{3/4} \qquad (1.1)$$

The paper by Aung, Fletcher and Sernas (1972) [2]was the first to define the significant parameters for this type of problem. Their definitions of the Nusselt and Rayleigh numbers, used in most papers published thereafter, are

$$\overline{Nu} = \frac{\overline{q''}\, b}{k(\overline{T}_{1/2} - T_o)} \qquad (1.2)$$

$$Ra'' = \frac{g\beta Pr\, b^5\, q''}{\nu^2 \quad k\, L_3} \qquad (1.3)$$

In the 80's, a renewed interest was shown in the field of natural convection as a cooling system. Jonhson (1986) [3] developed correlations for the use of natural convection as a cooling scheme for electronic equipment. He performed experiments and obtained data for a channel Rayleigh number in the range [15,100]. This is the region where densely-populated and highly-powered narrow-channel circuit

board applications occur.

His results were in good agreement with those of Aung [2],

$$Nu = 0.144\ Ra^{0.5}\ (\text{Fully developed limit})$$

$$Nu = 0.524\ Ra^{0.2}\ (\text{Single plate limit}) \qquad (1.4)$$

Additional correlations have been obtained recently. Examples include the work by Wirtz and Stutzman (1982) [4],

$$Nu = \frac{0.144\ Ra^{0.5}}{(1 + 0.0156\ Ra^{0.9})^{0.33}} \qquad (1.5)$$

by Bar-Cohen and Rohsenow (1984)[5],

$$Nu = \left(\frac{48}{Ra} + \frac{2.5}{Ra^{0.4}}\right)^{-0.5} \qquad (1.6)$$

and by Birnbier (1981) [6],

$$Nu = 0.20\ Ra^{0.31} \qquad (1.7)$$

Although many have studied the case of natural convection between two plates, the direct extension to consider free convection between a series of vertical plates, has not received much interest. Recently, Kim, Anand and Fletcher (1989) [7] published the results of experiments dealing with an array of vertical plates in open surroundings. Their results are presented in terms of temperature distribution in the channel, temperature distribution along the plates and maximum surface temperature. They also studied the effect of conduction in the wall on the average Nusselt number.

Most recently, Ramanathan and Kumar (1991) [8] have presented a new correlation for natural convection between heated vertical plates in an enclosure. Their results are given in terms of average Nusselt number and maximum temperature

$$Nu = \{\frac{185}{R^5} + (23\ Ra''^{-1.3} + 0.5\ Ra''^{-0.6})^{-1.25}\}^{0.2} \tag{1.8}$$

$$T_{max} = \left\{\left[\frac{R^2}{5} + \frac{R^4}{15}\right]^{-1.1} + 0.0122\ Ra''^{1.1}(1 + 0.0156\ Ra''^{0.9})^{-0.75}\right\}^{-0.4} \tag{1.9}$$

where R is the channel aspect ratio, L_3/b.

CHAPTER III: THEORETICAL FORMULATION

3.1 Mathematical formulation

The governing equations for this problem are derived from the basic laws of conservation of mass, momentum and energy. The seven geometrical parameters, shown in Figure 1, are H, L, a, L_1, L_2, b and L_3. To reduce the number of variables, the dimensionless ratios of, L_3/b, the enclosure aspect ratio, H/L_3 and the ratio H/L are used. The parameter, a, is fixed and L, and L_2 are not independent parameters since:

$$L=3a+2b+2L_2$$

and

$$H = 2\,L_1 + L_3$$

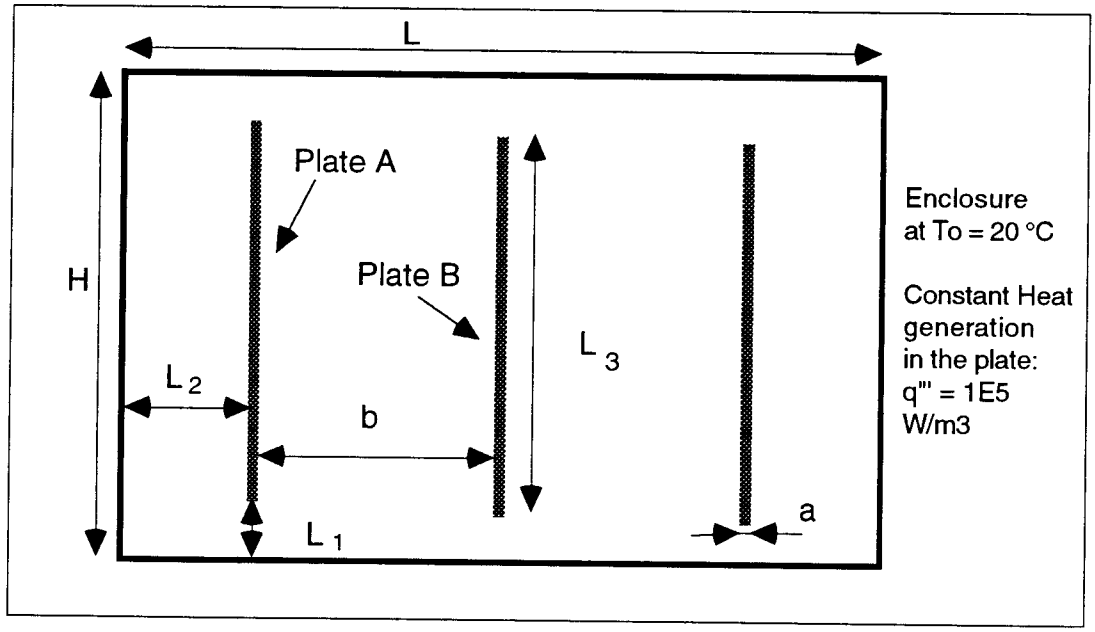

Figure 1: Geometrical configuration

The conditions to be considered are for laminar, incompressible, steady and two dimensional flow with no viscous dissipation of thermal energy. The heat transfer by radiation will be neglected in this study. The Boussinesq approximation is used by approximating the buoyancy force as:

$$\rho_o - \rho = \beta\,(t-t_o)\rho_o \qquad (3.1)$$

where β is the coefficient of volumetric expansion and, t, is the temperature.

The governing equations will be expressed in both dimensional and non-dimensional forms with the appropriate parameters defined.

Again referring to Figure 1 plate B will be fixed while the two other plates will be moved symmetrically away from plate B. The enclosure surfaces remain at the constant temperature, t_o, during all simulations. A uniform volumetric heat generation q''' will heat the plates, producing, for most configurations, a uniform heat flux on each plate surface.

Since the problem is symmetrical, only the left half of the problem will be analyzed to optimize grid size and the computation time. The boundary conditions at the center line (right end of our half problem) will be written as:

$$U = 0, \quad \frac{\partial V}{\partial X} = 0, \quad \frac{\partial T}{\partial X} = 0 \qquad (3.2)$$

The governing equations are;
continuity:

$$\frac{\partial u}{\partial x} + \frac{\partial v}{\partial y} = 0 \qquad (3.3)$$

x-momentum:

$$u\frac{\partial u}{\partial x} + v\frac{\partial u}{\partial y} = -\frac{1}{\rho}\frac{\partial p}{\partial x} + \nu\left(\frac{\partial^2 u}{\partial x^2} + \frac{\partial^2 u}{\partial y^2}\right) \tag{3.4}$$

y-momentum:

$$u\frac{\partial v}{\partial x} + v\frac{\partial v}{\partial y} = \nu\left(\frac{\partial^2 v}{\partial x^1} + \frac{\partial^1 1}{\partial y^2}\right) + \beta g\,(t-t_o) \tag{3.5}$$

energy:

$$u\frac{\partial t}{\partial x} + v\frac{\partial t}{\partial y} = \alpha\left(\frac{\partial^2 t}{\partial x^2} + \frac{\partial^2 t}{\partial y^2}\right) \tag{3.6}$$

using

$$p = \rho\, R\, t \tag{3.7}$$

$$\frac{dp_o}{dy} = -\rho_o g \tag{3.8}$$

and

$$\rho_o - \rho = \beta\,(t-t_o)\,\rho_o \tag{3.9}$$

where

$$\beta = -\frac{1}{\rho}\left(\frac{\partial \rho}{\partial t}\right)_p \tag{3.10}$$

Using the following dimensionless variables, with b as the reference length and t_o as the reference temperature

$$U = u\frac{b}{\nu} \qquad V = v\frac{b}{\nu} \tag{3.11}$$

$$X = \frac{x-L_2}{b} \qquad Y = \frac{y-L_1}{b} \tag{3.12}$$

$$P = \frac{pb^2}{\rho\nu^2} \qquad T = \frac{t-t_o}{q'' b/k} \tag{3.13}$$

we obtain the following dimensionless equations,
continuity:

$$\frac{\partial U}{\partial X} + \frac{\partial V}{\partial Y} = 0 \tag{3.14}$$

X-momentum:

$$U\frac{\partial U}{\partial X} + V\frac{\partial U}{\partial Y} = -\frac{\partial P}{\partial X} + \frac{\partial^2 U}{\partial X^2} + \frac{\partial^2 U}{\partial Y^2} \tag{3.15}$$

Y-momentum:

$$U\frac{\partial V}{\partial X} + V\frac{\partial V}{\partial Y} = \frac{\partial^2 V}{\partial X^2} + \frac{\partial^2 V}{\partial Y^2} + Gr\,T \tag{3.16}$$

energy:

$$U\frac{\partial T}{\partial X} + V\frac{\partial T}{\partial Y} = \frac{1}{Pr}\left(\frac{\partial^2 T}{\partial X^2} + \frac{\partial^2 T}{\partial Y^2}\right) \tag{3.17}$$

where:

$$Pr = \frac{\nu}{\alpha} \qquad Gr = \frac{gb}{\nu^2}\frac{q'' b^4}{k} \tag{3.18}$$

Two additional ratios are required to compute the Nusselt number and the Rayleigh number. These are the heat flux ratio and temperature ratio; defined as

$$r_t = \frac{T_1 - T_0}{T_2 - T_0} \tag{3.19}$$

$$r_h = \frac{q_1}{q_2} \tag{3.20}$$

3.2 Quantities of interest

The maximum non-dimensional temperature on each plate, T_{max}, is the most important parameter for design. In addition we are interested in the following parameters

- Independent parameters

L_3/b, the channel aspect ratio

- Dependent parameters

$Nu = \frac{\overline{q''}\, b}{(\bar{t} - t_o)\, k}$, the average Nusselt Number in the channel, and

$Ra'' = \frac{gb}{k\nu\alpha}\overline{q''}\, b^5$ the average channel Rayleigh number

3.3 Numerical formulation: the Tempest code

Calculations in this thesis were made using the public-domain computer code, TEMPEST by Trent and Eyler (1991) [9], developed at Battelle, Pacific Northwest Laboratories.

TEMPEST stands for Transient Energy Momentum and Pressure Equations Solution in three dimensions.

TEMPEST numerical procedures are based on a semi-implicit finite difference method. The momentum equations are solved explicitly, the continuity and pressure solutions are solved implicitly. The energy equation is solved for both the fluid and the solid regions and obtained implicitly. TEMPEST will solve single phase, incompressible flows using the Boussinesq assumptions.

Since the geometry of this problem is rectangular, a Cartesian coordinate system (x,y,z) is appropriate and was, therefore, chosen. The TEMPEST coordinate system is shown in Figure 2 Gravitational acceleration is specified in the usual form.

$$\vec{g} = -g\vec{z} = -9.8\,\vec{z} \qquad (3.21)$$

TEMPEST simulations operate under the following conditions:

- Body forces other than gravity are not considered
- Fluids are Newtonian.
- Viscous dissipation is neglected
- The Boussinesq approximation holds (i.e. $\frac{\Delta\rho}{\rho_o} \ll 1$). This approximation is commonly used in natural convection.

All of the above conditions are valid for this problem and TEMPEST should, therefore, generate proper results.

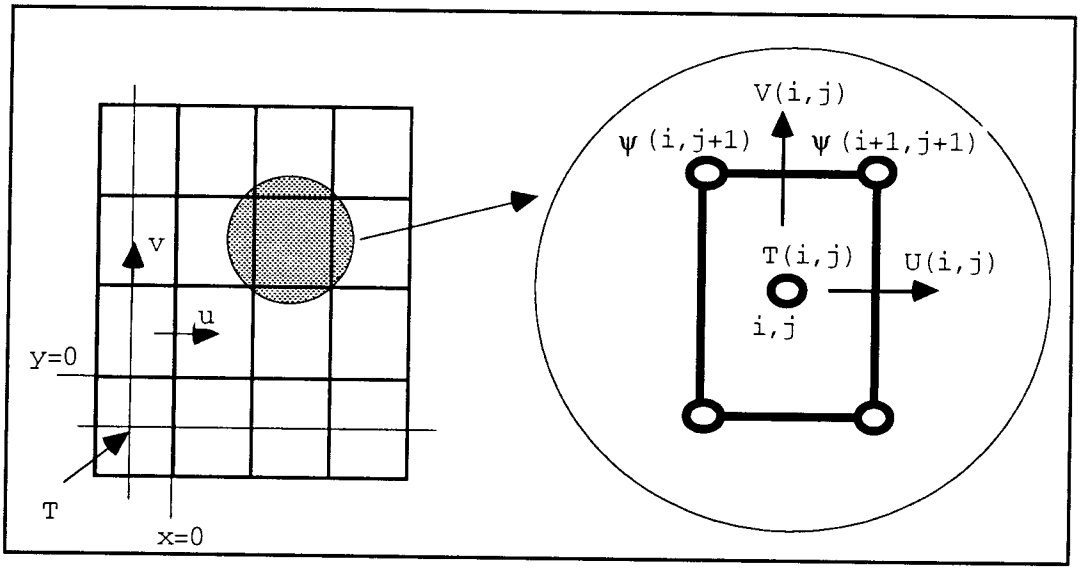

Figure 2: TEMPEST coordinate system

3.3.1 Solution procedure

TEMPEST solves all governing equations sequentially using a semi-implicit time marching difference procedure. At each time step, the momentum equations are solved explicitly whereas the pressure equations, and temperature equations are solved implicitly. The solution proceeds in the three phases as follows:

- Phase I- Tilde phase. The three momentum equations are advanced in time ($t + \Delta t$) to obtain approximate (tilde) velocities, based on the previous-time values of pressure and density, P and ρ . Although these values of the velocity components satisfy the momentum equations based on current values of P and ρ , continuity will not usually be satisfied.
- Phase II - Implicit phase. The velocity components and pressure corrections (U',V',W' and P') are obtained such

that the equations

$$U^{n+1} = \tilde{U} + U' \tag{3.22}$$

$$V^{n+1} = \tilde{V} + V' \tag{3.23}$$

$$W^{n+1} = \tilde{W} + W' \tag{3.24}$$

$$P^{n+1} = \tilde{P} + P' \tag{3.25}$$

satisfy continuity.

- Phase III - Scalar phase. Using the previously computed values of U^{n+1}, V^{n+1}, and W^{n+1}, the advanced-time $(t + \Delta t)$ values of temperature, T^{n+1}, and other scalar quantities are computed as required.

The solution is advanced step by step in time by continued application of the above three solution phases.

3.3.2 Computational cell structure

The grid choice can have a great influence on both the computational time and the accuracy of the results. TEMPEST allows the creation of a non-uniform cell structure in all directions. Since we have dealt with a 2D problem, the Z direction, indexed by k, was left out.

Different tests were run to define a good compromise between accuracy and total computational time cost. Those cases are:

1. Constant grid spacing in both directions
2. Variable grid spacing in the x-direction, constant grid spacing in the y direction
3 Variable grid spacing in both directions.

The accuracy was determined by examining the average Nusselt number, streamlines, and isotherms. Quite surprisingly, the difference in the average Nusselt number was very small. All of these grid configurations produced average Nusselt numbers within less than 10%

for all configurations. The Nusselt number consideration was, thus, not the critical parameter in deciding the grid configuration to be used.

Streamlines and isotherms in the enclosure displayed major differences with different grid configurations as shown by Figures 3, 4, and 5.

As shown in Figure 3, the use of a large constant Δx produces considerable errors at the plate faces. When the channel is small, the number of cells that model the flow behavior is too small to represent accurately the real behavior. Boundary layer effects are not well represented because of the steep temperature gradients at the plates surfaces. This is one reason why a greater number of cells with a small Δx should be used in this region. It also appears that the wall itself is misrepresented using only one cell since the flux removed from each face will vary.

Figure 4 illustrates the importance of the choice of Δy. The isotherms at the entrance of the channel clearly show that a finer grid is needed in this area. This is necessary to account for the rapid change in temperature at this location. Obviously, since temperature differences drive the flow, the same accuracy is needed to represent the flow pattern. The streamline plot, Figure 5, shows that, next to the bottom and top walls, where the velocity gradient changes drastically, a smaller grid is needed to model the flow in a more realistic fashion. The computational time would be very large if a small uniform grid size were chosen. Therefore, to keep computational time reasonable (about three hours per simulation) and to obtain sufficient accuracy at key locations in the region of interest, a variable grid spacing was used. A fine mesh was used next to the enclosure walls, the plates faces and the plate boundaries. The detail of the grid is shown in appendix B.

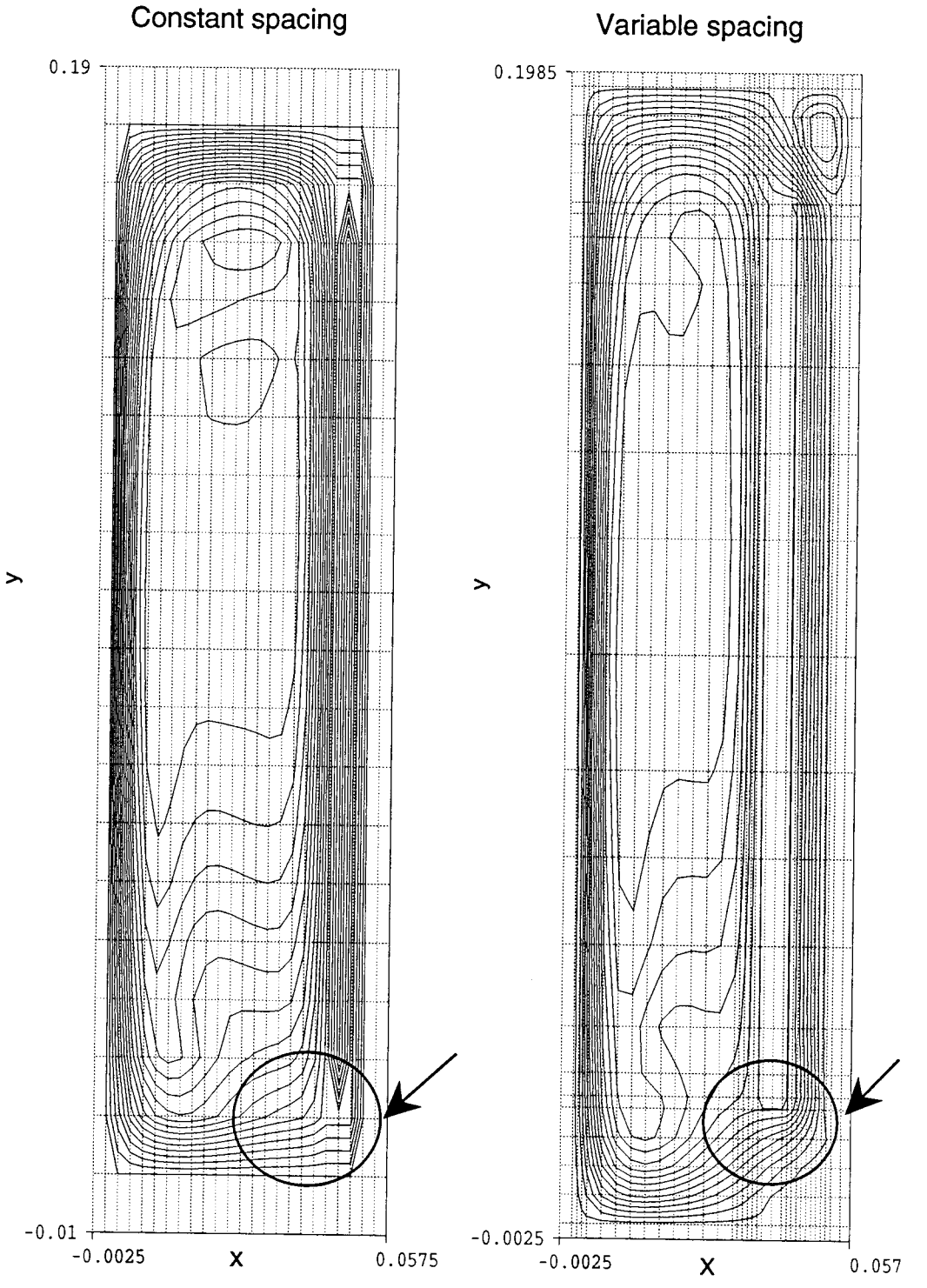

Figure 3: Influence of variable grid in the x direction, regions of comparison for grid spacing are highlighted

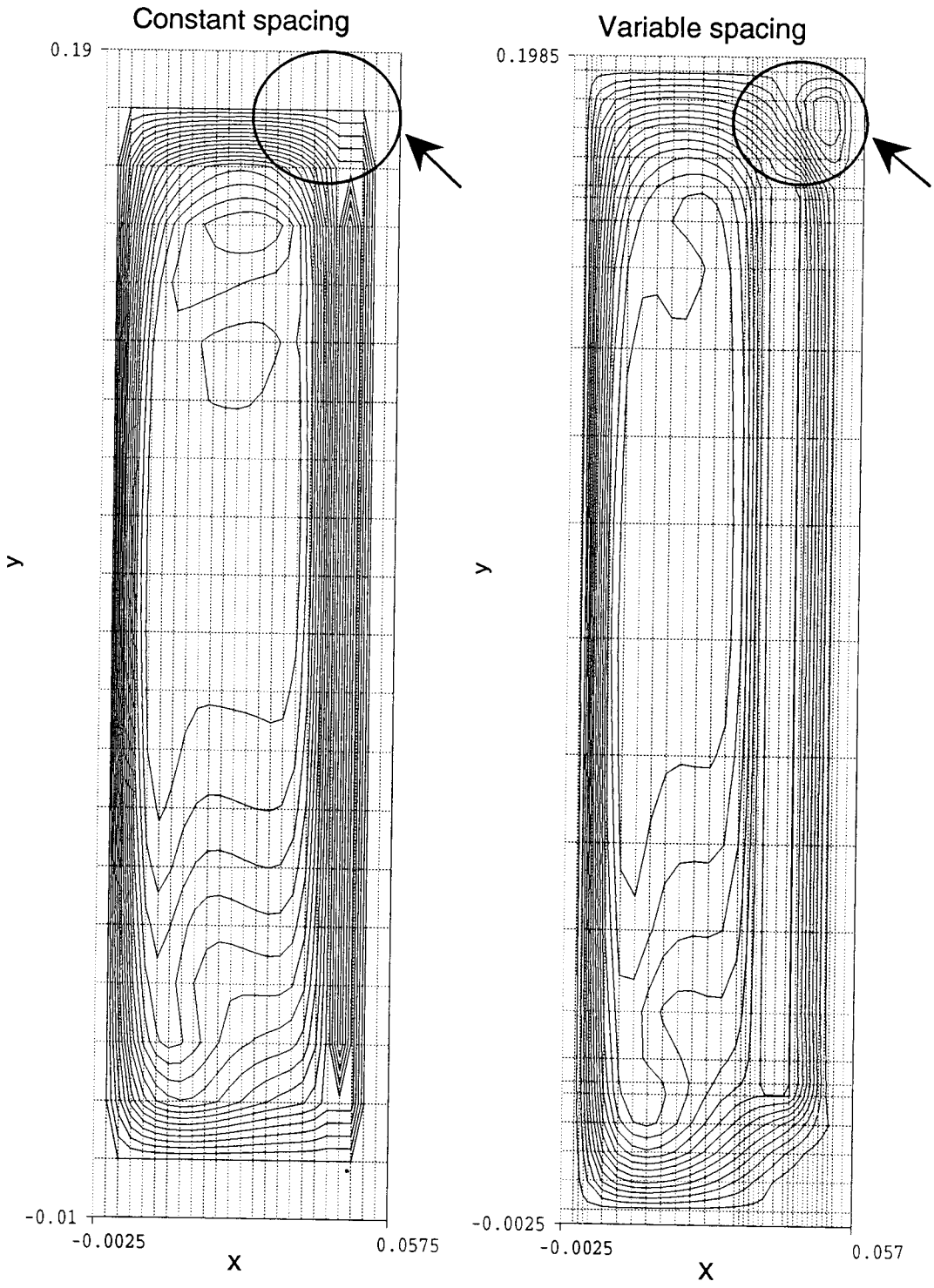

Figure 4: Influence of variable grid in the y direction, regions of comparison for grid spacing are highlighted

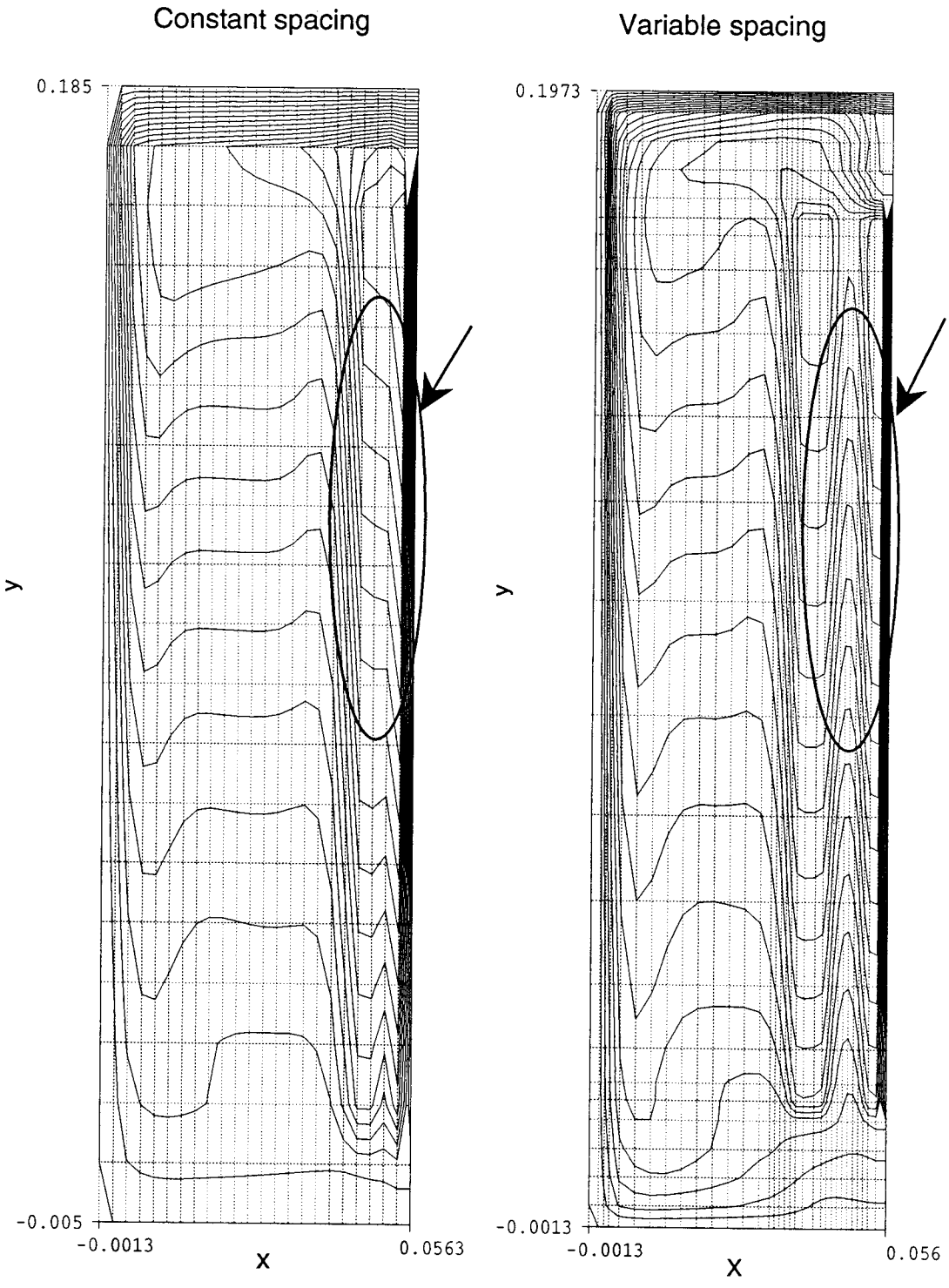

Figure 5: Influence of variable grid, regions of comparison for grid spacing are highlighted

CHAPTER IV: NUMERICAL SIMULATIONS

4.1 Installation of Tempest

TEMPEST is an ANSI Fortran 77 code. Since the computer used in this work, a NeXT workstation, has no Fortran compile,; an alternate means had to be found. The AT&T code, f2c [10], that converts an ANSI Fortran code to a C code was used. Thanks to the great support team at AT&T and the competence of the local system administrator, f2c was successfully installed on the NeXT after encountering a few compatibility problems specific to the NeXT.

All of the TEMPEST subroutines except for one accessing the time, date, and CPU time were successfully converted. All of these subroutines were replaced by dummy subroutines, thus, the version of TEMPEST used doesn't provide information about the total CPU time used in the process.

4.2 Description of different simulations

In order to obtain a correlation of the form Nu= f (Ra"), the moving plate position was changed nineteen times and a TEMPEST simulation obtained for each case. In each case, values of L, H, L_1, L_2, L_3, and q''' were held constant; the only variable was the channel width, b. One group of nineteen simulations will be referred to as a set.

In order to define the time at which steady state was reached, velocity and temperature values generated every five seconds up to 200 seconds for case x.1, x.6, x.12 and x.19 were recorded. Steady state was determined for these cases when no further variation with time was observed. After the time required to achieve steady state was

determined, the other simulations were run for that time and output was only printed out at the end.

The maximum pressure iteration was set to 50 after trying different values. This gives perfectly symmetric results on the full configuration simulation. The temperature and both velocities are generated as output in both a ASCII file and a binary postprocessing file.

4.3 Postprocessing procedure

A postprocessing code was written to generate results in a more visual or standard form than the raw results provide by TEMPEST. This code creates files for visualizing the temperature profiles, the streamlines, the temperature profile in the channel and along the plates, the velocity profile in the channel and the Nusselt and Rayleigh numbers.

4.3.1 Streamlines and isotherms

The streamlines are computed using a finite difference procedure on the y-component of the velocity, v. The streamfunction ψ is defined as

$$u = \frac{\partial \psi}{\partial y} \tag{4.1}$$

$$v = -\frac{\partial \psi}{\partial x} \tag{4.2}$$

Expressing v in finite difference form and referring to the grid shown in Figure 6, we have

$$v_{i,j} = -\frac{\psi_{i,j} - \psi_{i-1,j}}{\Delta x_i} \tag{4.3}$$

and thus

$$\psi_{i,j} = \psi_{i-1,j} - v_{i,j}\Delta x_i \qquad (4.4)$$

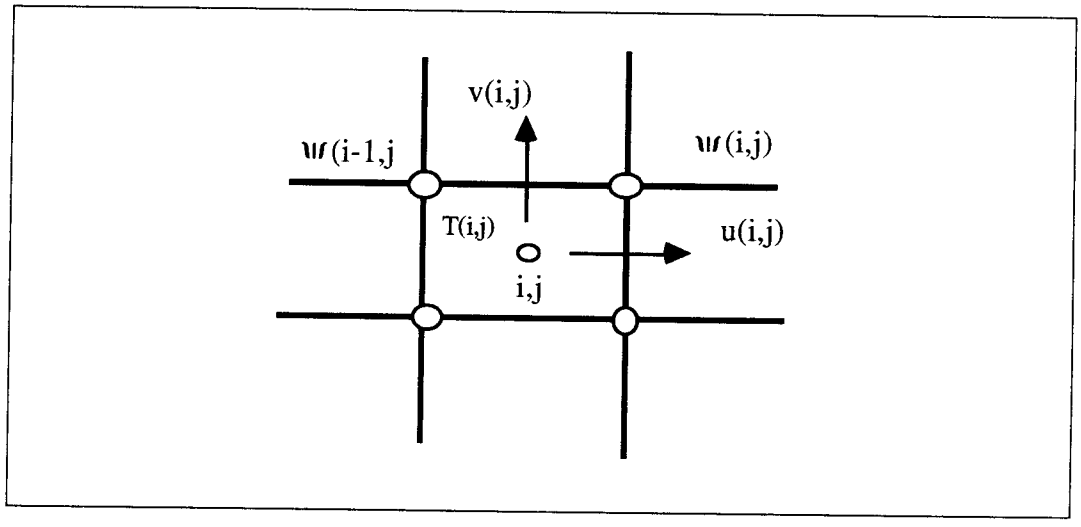

Figure 6: Grid system for the streamfunctions calculation

The boundary conditions are

$$\psi_{1,j} = 0 \qquad (4.5)$$

and

$$v_{i,n} = 0 \qquad (4.6)$$

A marching procedure was then used to compute values for ψ, line by line, beginning from the bottom line. To maintain accuracy and also to satisfy requirements (NXcontour has a good resolution when its contour level are greater than 1) of the contouring program, the stream function values were multiplied by 10^4.

To plot the isotherms, values of temperature are needed. Since this is a direct output from TEMPEST, it was only necessary to create

a file in a format readable by the plotting software.

In addition, Figure 6 shows clearly that the velocity, temperature and the streamfunction are all located at different points on the grid. Because a non-uniform grid was used, it was necessary to compute specific temperature and streamfunction grids for input to the graphing software.

The graphical representation of the streamlines was done on the NeXT with NXcontour [11], a color contouring program.

4.3.2 Nusselt and Rayleigh number computation

To compute an average Nusselt number, a reference length and reference temperature were defined. Since we were studying the effect of the channel aspect ratio, the reference length used is, b, the channel width. The Nusselt number then characterizes the heat exchange between the two plates in the channel.

Choosing a reference temperature is a much more difficult task. A few choices were possible – the entrance temperature in the middle of the channel, the temperature in the middle of the channel at the channel midheight, or the ambient fixed temperature on the outside of the enclosure.

Since our purpose was to develop a correlation to help in the design of such enclosures, the two first choices were eliminated because those two temperature were not known a priori. Hence, the ambient temperature, $t_{o,}$ was chosen as the reference temperature.

Expressing the average Nusselt number as:

$$\overline{Nu} = \frac{\bar{q}\, b}{(\bar{t} - t_o)\, k} \qquad (4.7)$$

where

$$\bar{q} = \frac{q_1 + q_2}{2} \tag{4.8}$$

and,

$$\bar{t} = \frac{t_{1,1/2} + t_{2,1/2}}{2} \tag{4.9}$$

and using the non-dimensional numbers defined in page 8, the average Nusselt number was then computed as:

$$Nu = \frac{1 + r_h}{1 + r_t} \frac{1}{T_2} \tag{4.10}$$

Similarly, the channel Rayleigh number was computed using non-dimensional numbers, as defined in §3.2

$$Ra'' = \frac{g\beta}{\nu^2} \frac{q_2 b^5 Pr}{L_3 k} \frac{1 + r_h}{2} \tag{4.11}$$

One of the difficulties in obtaining this number comes is because the variables q_1 and q_2 are to be computed. Because of conduction effects in the plate, the heat flux on each face of the plates will not be strictly uniform and will show significant variations with plate location.

The heat fluxes on each face, must then be computed to yield an average heat flux. Using Fourier's law

$$q'' = - k \frac{\partial t}{\partial y}\Big)_{x=0} \tag{4.12}$$

the average flux, q_i, was computed as

$$q_i'' = - \frac{2}{L_3} \sum_j \frac{t_{j,i,air} - t_{j,i,face}}{\frac{\Delta x_{i,air}}{k_{air}} + \frac{\Delta x_{i,face}}{k_{face}}} \Delta y_j \tag{4.13}$$

4.3.3 Temperature profiles

The temperature is the major concern for design purposes. It is therefore necessary to know the temperature profiles in the plates. Non-dimensional temperature variations on plate A and B were stored in different output files. The profiles were then generated using the Macintosh graphics package Kaleidagraph [12].

4.3.4 Velocity profiles

The velocity profile in the channel provides us with very important information about the flow. Among other information the velocity profile can confirm the choice of the mesh size by including enough points in the boundary layer.

The non-dimensional velocity, V, at the entrance, mid-height and the exit of the channel was stored in a separate file. Profiles were then generated with Kaleidagraph.

4.3.5 Correlation procedure

Churchill and Usagi (1972) [13] developed a technique to correlate experimental data. This method has been used by numerous researchers to correlate the Nusselt number as a function of the channel Rayleigh number.

Churchill and Usagi showed, that if an arbitrary function, $y_{1,}$ is a function of z_1, and the functional relationship between these two variables is characterized by two asymptotic limits for low and high values of z_1, then using the principle of superposition, y_1 may be expressed as

$$y_1 = \left(\left(Az_1^p\right)^n + \left(Bz_1^q\right)^n\right)^{1/n} \qquad (4.14)$$

where

$$y_1 \rightarrow A\, z_1^p \quad \text{as } z_1 \rightarrow 0$$

$$y_1 \rightarrow B\, z_1^q \quad \text{as } z_1 \rightarrow \infty$$

$$n > 0, \quad \text{if } p < q$$

4.3.6 Optimum spacing , b_{opt}

Optimizing the channel width b can be done by answering one of the following two questions

1. For what channel width, b, is the maximum plate temperature T_{max} minimum?

2. For what channel width, b, is total heat dissipation per unit-average-temperature-increase a maximum?

The first question can be answered easily by plotting T_{max} as a function of b. A value for b_{opt} is then found for that configuration. The drawback of this method is that, for each new configuration, a new set of simulations must be performed to find the new value, b_{opt}.

The second question can be answered by maximizing $Q_T / \Delta T$ with respect to b.

Looking at the results obtained from the first method as shown in Figure 26, we observe that the optimum occurs in a range where the fluxes q_1'', q_2'', and q_3'' are all equal. From this observation, the ratio $Q_T / \Delta T$ can be expressed as a function of the average Nusselt number and the aspect ratio

$$Q = 3\, L_3\, a\, q'' = 3\, L_3\, a\, Nu\, \Delta T\, k / b$$

$$\Rightarrow Q / \Delta T = f(Nu.L_3/b)$$

CHAPTER V: ANALYSIS OF RESULTS

5.1 Steady state determination

To determine the steady state, the temperature and velocity results were monitored at various grid locations for different values of the parameter b. Figures 7, 8 and 9 respectively show the variation of temperature, the x-component velocity, u , and the y-component velocity, v, with time at the first cell beneath plate A – denoted with subscript 1– and at the first cell above plate B – with subscript 2.

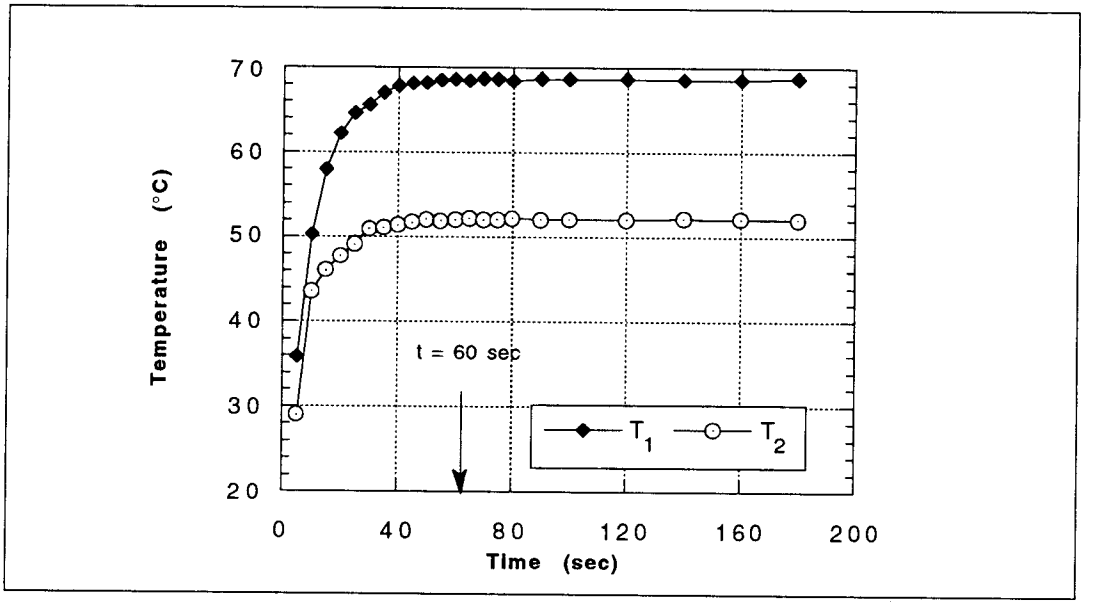

Figure 7: Determination of steady state — Temperature variations above plate A and below plate B

Observing Figure 7 it appears that steady state occurs for approximately t > 60 sec. However, an examinination of the velocity variation shows that steady state is not reached for a much longer time. Actually, steady state is never strictly observed, instead the velocity oscillates around a constant value. This average value reaches a constant after a reasonable period of time. Steady state was considered reached when the variations around that mean became small.

Using these rules for the example case shown, steady state was reached at t > 100 sec. All results observed in this study are for output data recorded from TEMPEST at simulation time t = 100 sec.

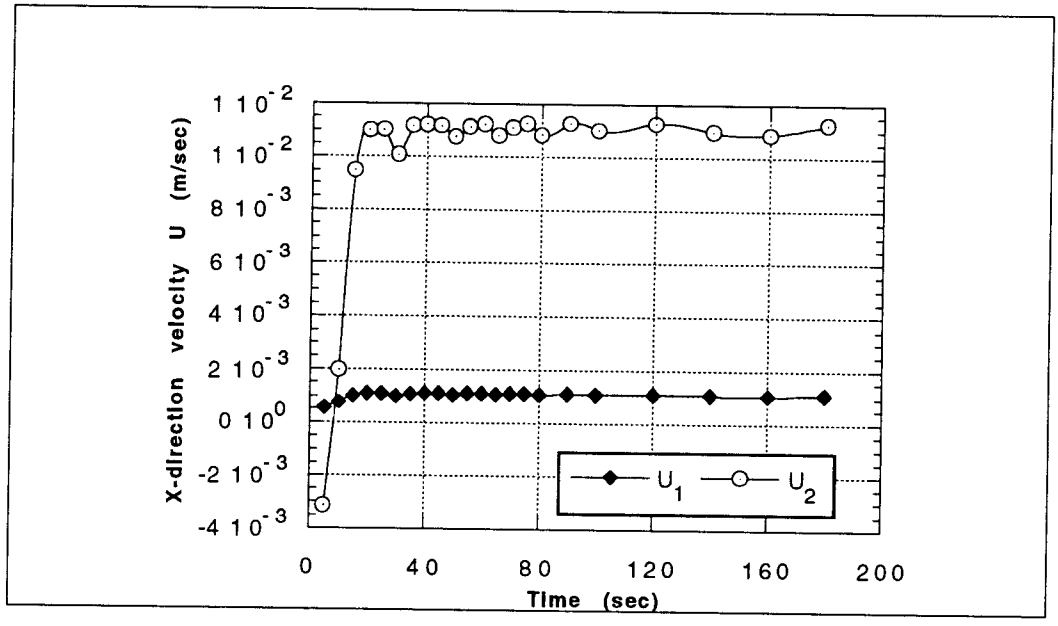

Figure 8: Steady state determination — x-component velocity, u, variation with time

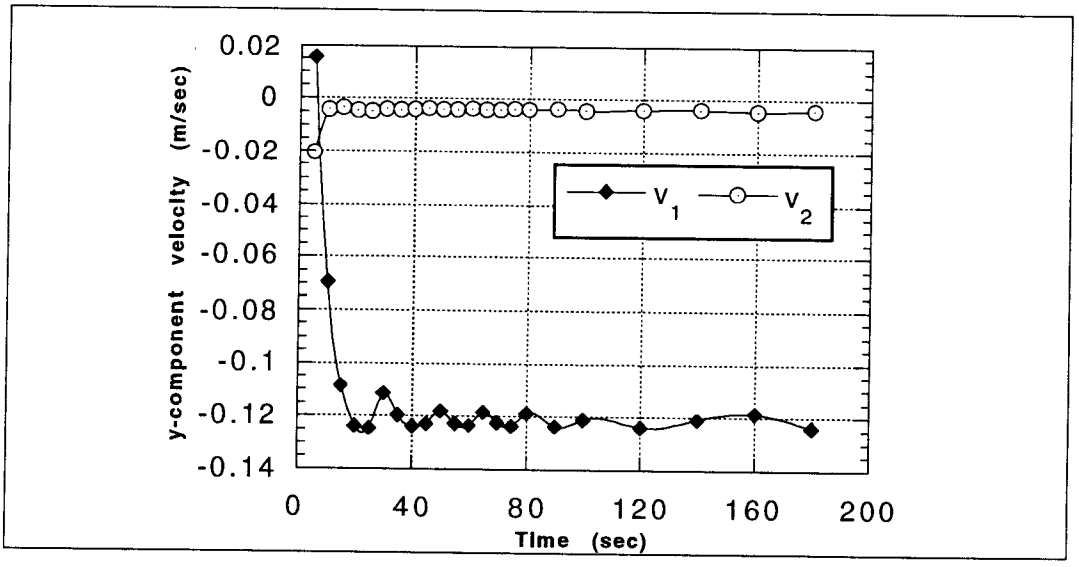

Figure 9: Steady state determination — variation of the y-component velocity with time

5.2 Nusselt number

The average Nusselt number computed is the average non-dimensional temperature gradient in the channel. This number is of interest since it is directly related to the cooling efficiency of the channel.

Figure 10 shows the variation of the average Nusselt number, computed at midheight, as a function of the channel Rayleigh number, Ra", for three simulation sets. Each set was performed with a different heat generation input (10^5, 10^4, and 10^3 W/m^3). The channel Rayleigh number is a function of the heat flux and of the channel width. These results show that b and q''' both have the same final effects on the Nusselt number — either a change in b or a change in q''' produce the same change in Ra" resulting in the same variation in Nu.

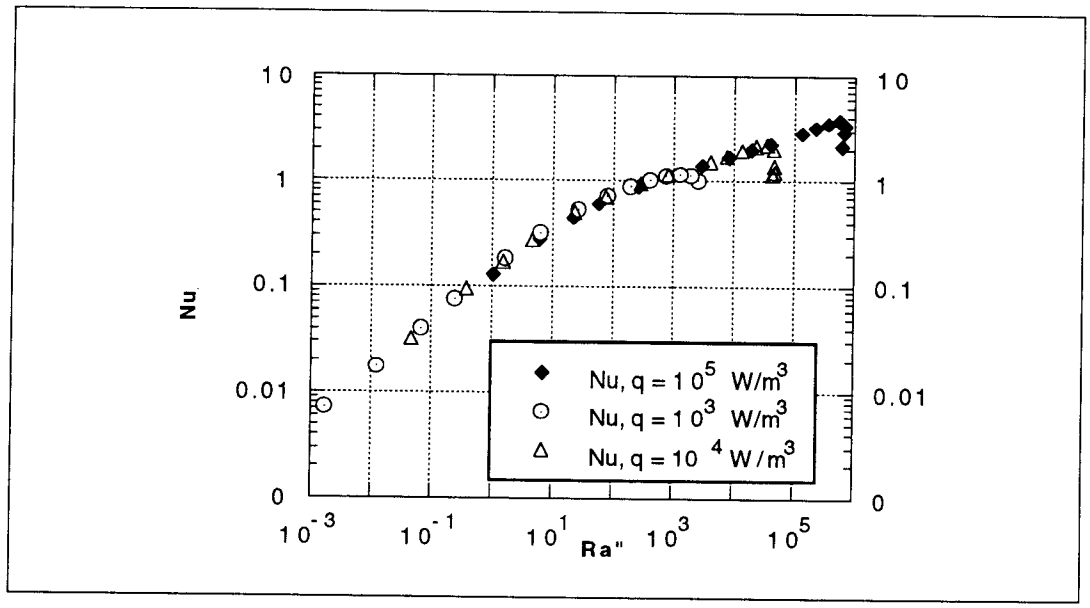

Figure 10: Average Nusselt number as a function of Ra"

Figure 10 suggests that the channel Rayleigh number variation can be divided into three ranges: a lower range [0,10] in which the flow is laminar and fully developed, an upper range [300, 10^6] where a behavior similar to that of the single plate occurs, and an intermediate range [10,300] where a transition from the first phenomenon to the second takes place. In the lower range, Nu is a function of $Ra"^{1/2}$; in the higher range, Nu is a function of $Ra"^{1/5}$.

The results presented in Figure 10 also show an unusual phenomenon that occurs for the five last simulations in each set. This anomalous behavior corresponds to higher values of b, or more clearly, occurs when plate A comes very close to the constant temperature wall. For these cases, the Nusselt number drops very rapidly. In this case the gap between the wall and the plates being so small, the main heat transfer mode becomes conduction. This being so, the temperature

on the left face of plate A tends to be very close to the constant wall temperature, thereby stopping the flow. Since we are modeling convection effects, it is reasonable to neglect these points for determining a correlation. Figure 11 shows the results of all three sets of simulations except for those points described above. Using these data, a correlation was computed using the Churchill and Usagi [14] algorithm.

From the TEMPEST output, the lower and upper asymptotic correlations can be expressed as

$$Nu = 0.131\ Ra''^{0.5} \tag{5.1}$$

$$Nu = 0.277\ Ra''^{0.2} \tag{5.2}$$

The Nusselt number can then be expressed as in equation (4.14). The best value of the exponent, n, can be evaluated by comparing the previous equation with the data obtained with TEMPEST. Churchill and Usagi suggested that this could be best done by rewriting b equation (4.14) in the form:

$$\frac{y}{Az^p} = \left[1 + \left(\frac{Bz^{q-p}}{A}\right)^n\right]^{1/n} \tag{5.3}$$

$$Y = (1 + Z^n)^{1/n} \tag{5.4}$$

and then comparing the data with the curve of Y versus Z. Alternatively, when the precise value of Y is known at Z=1, n can be determined directly as ln2/lnY. Following this procedure, a value of n=-6 was obtained.

The Nusselt number correlation as a function of the channel Rayleigh number is then

$$Nu = \left(\left(0.131Ra''^{0.5}\right)^{-6} + \left(0.278\ Ra''^{0.2}\right)^{-6}\right)^{-1/6} \tag{5.5}$$

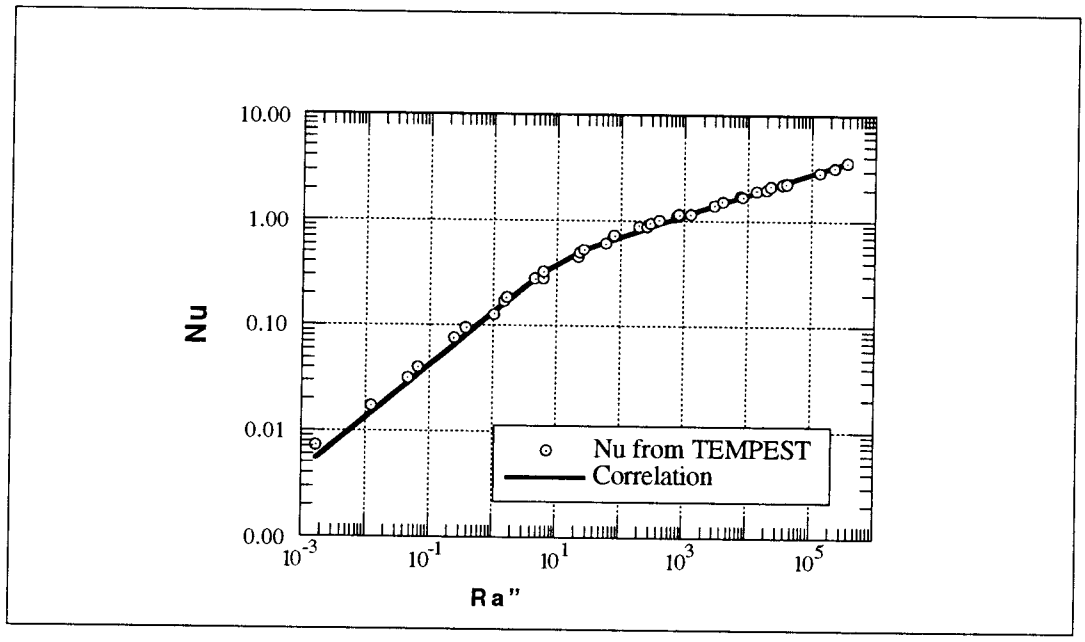

Figure 11: Correlation for the average Nusselt number

A plot of the residual is shown in Figure 12. This clearly shows that even though the correlation seems to be graphically better in the higher Ra" range, the opposite is true since the residual tends to grow as Ra" grows.

Figure 13 shows a comparison of the correlation obtained by Wirtz and Stutzman [5] for two vertical plates heated by a uniform equal flux. In the lower range of Ra", the two plots match very well. This is the fully-developed region. The boundary layers merge after a short length and the velocity profile becomes parabolic. In this region, flows have the same hydrodynamic properties and therefore should have the same heat transfer properties. The good agreement between these results shows that the entrance and exit lengths, where the flow

deviates from its fully developed characteristics, are negligible.

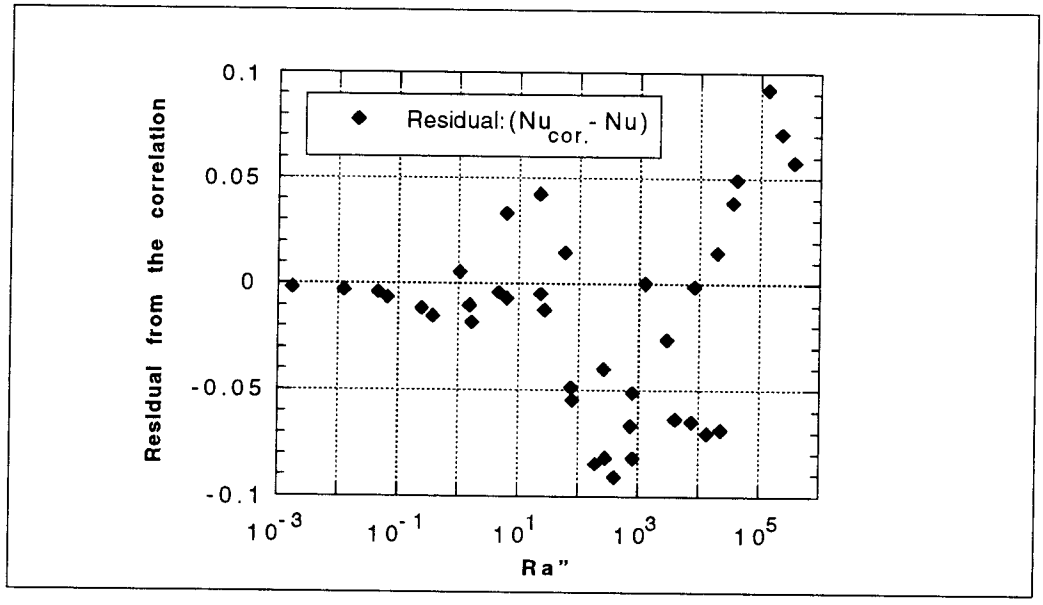

Figure 12: Residuals from the correlation as function of the channel Rayleigh number

In the higher range, both curves approach separate asymptotic limits. The enclosure appears to lower the Nusselt number by a constant value. In both cases, $Nu \sim Ra''^{1/5}$ which corresponds to the single-plate limit. As expected, for the same heat input, q''', and the same channel width, b, the plate temperature in the enclosure is higher than the one with no enclosure since the Nusselt number for the enclosure case is lower than the other. No good explanation can be given to explain the phenomenon causing the difference between these plots. More simulations, changing the ratio H/L and H/L_3, would aid in

describing this variation.

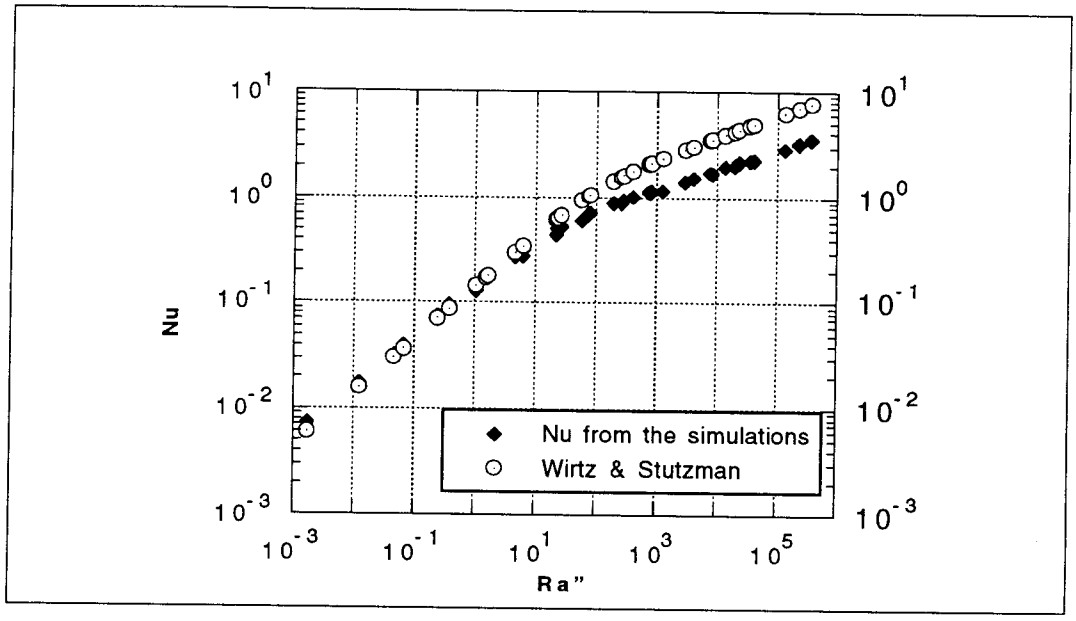

Figure 13: Comparison with Wirtz & Stutzman correlation for a channel without enclosure

The other limiting case, the pure enclosure, was not compared since only one point could be obtained from the unique configuration that was simulated.

5.3 Temperature in the plates

To explain the variations of the temperature in plates A and B, the non-dimensional temperature (inverse of the local Nusselt number) profiles have been plotted as functions of the non-dimensional position about the plate. These profiles are shown for four different values of channel aspect ratio, Γ. In Figure 14, $\Gamma = 3.6$, which is the case when plate A is as close as possible to the constant-temperature wall. In Figures 15 and 16, Γ is 4.6 and 9.75, respectively and, b is about 2L/3

and L/3. Figure 17 shows the temperature profiles for $\Gamma = 52$, that is when plate A is as close as possible to plate B.

All of these cases display similar trends, the temperature increases height, reaching a maximum before decreasing slightly near the top. Three types of behavior appear to occur.

In Figure 14, the temperature of plate A is very different from the other cases. Two main differences are: 1) its temperature is much lower than the temperature in plate B, and 2) the profile is very flat, having a maximum near the middle of the plate. This variation shows that, for this value of b, the convective mode of heat transfer has become negligible relative to conduction. Convection tends to shift the maximum temperature in the plate to the upper end. This shift of the maximum toward the middle of the plates, indicates that the flow is going downward along the right face of plate A, in a circulation cell.

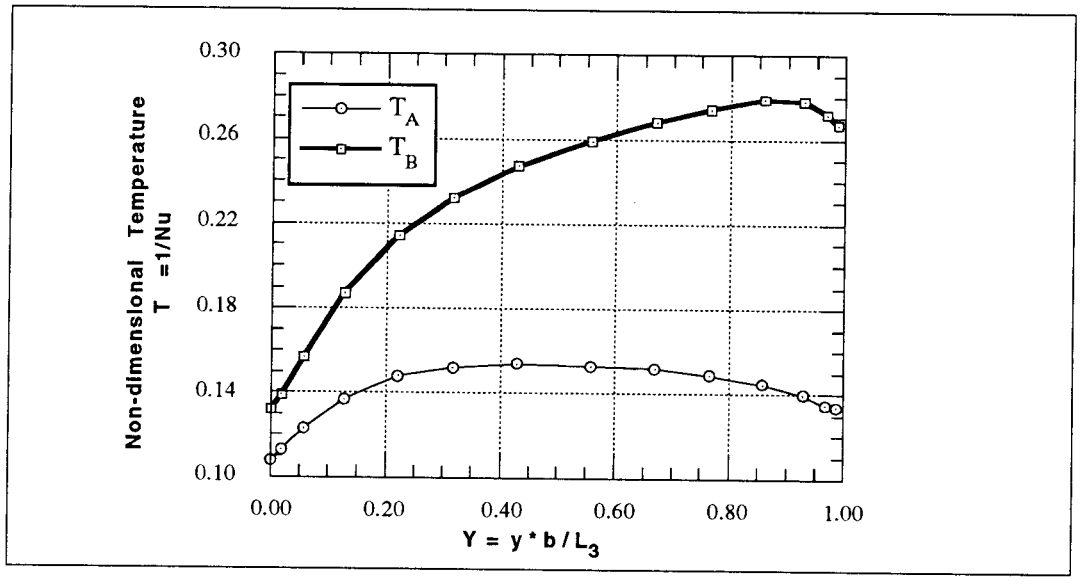

Figure 14: Non-dimensional temperature profile in the plates for $\Gamma = 3.6$

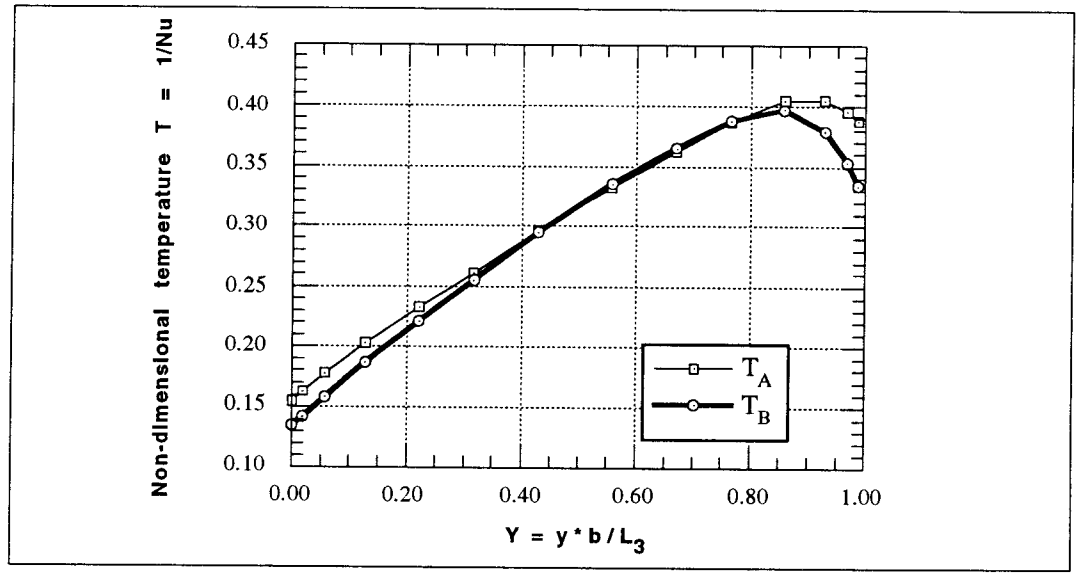

Figure 15: Non-dimensional temperature profile in the plates for $\Gamma = 4.6$

Figures 15 and 16 show similar behavior. The temperatures rise to a maximum before decreasing. Temperature in plate B reaches a maximum at a lower height than for plate A. Also, the temperature in plate B drops to a lower value than in the case for plate A. The maximum temperature in plate A is almost the same as the temperature at the top of the plate. Toward the top of the plate, cooling seems to be much more efficient for plate B than for plate A. It is also interesting to note that the maximum temperature in plate A decreases with b as soon as convective heat transfer effects become dominant. Notice also that the plate temperature increases as b decreases.

Figure 17 shows temperature profiles in plates A and B when the flow is fully developed. For this case, both maxima occur at the top of the plate. The temperature in plate B increases with height, more

rapidly than in plate A, resulting in a greater maximum temperature in plate B. This difference of cooling performance can be explained by the fact that plate A is cooled very efficiently from its left face.

A general observation is that both plates behave very similarly; their maximum temperatures increase as their locations occur nearer the top.

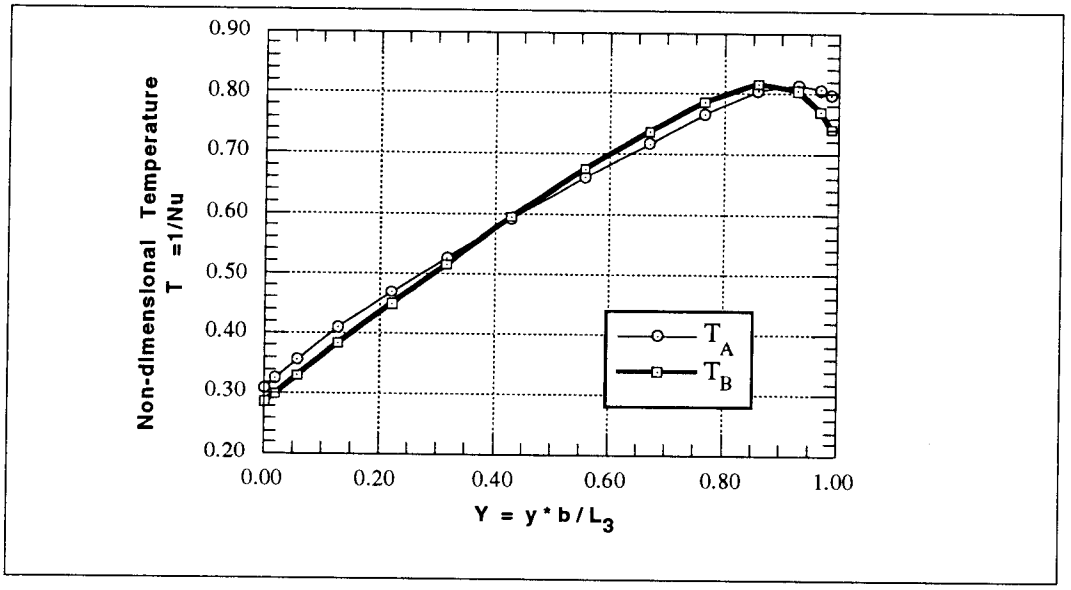

Figure 16: Non-dimensional temperature profile in the plates for $\Gamma = 9.75$

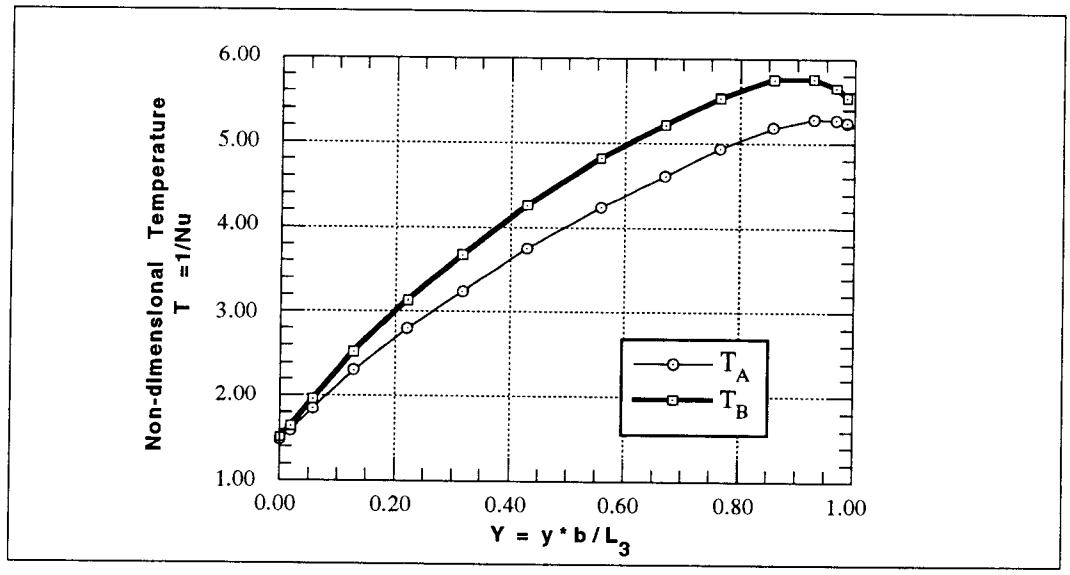

Figure 17: Non-dimensional temperature profile in the plates for $\Gamma = 52$

5.4 Velocity in the channel

Plotting velocity profiles in the channel provides both qualitative and quantitative information on the flow patterns. It also indicates how good or bad the choice of the grid size was for the numerical computation.

Figures 18, 19, 20 and 21 show non-dimensional velocity profiles at three locations in the channel — the entrance, Y=0, midheight, Y=0.49, and near the exit Y=0.98 — for the four channel aspect ratios used previously — Γ = 3.6, 4.6, 9.75 and 52.

Here again, three pattern types appear. Figure 18 shows a weak boundary layer at the entrance of the channel. The midheight and exit profile, however, show profiles characteristic of enclosures — the cold side flow (plate A) goes down while the hot side flow (plate B) rises.

From these results, we expect to see a circulation cell in the top part of the channel.

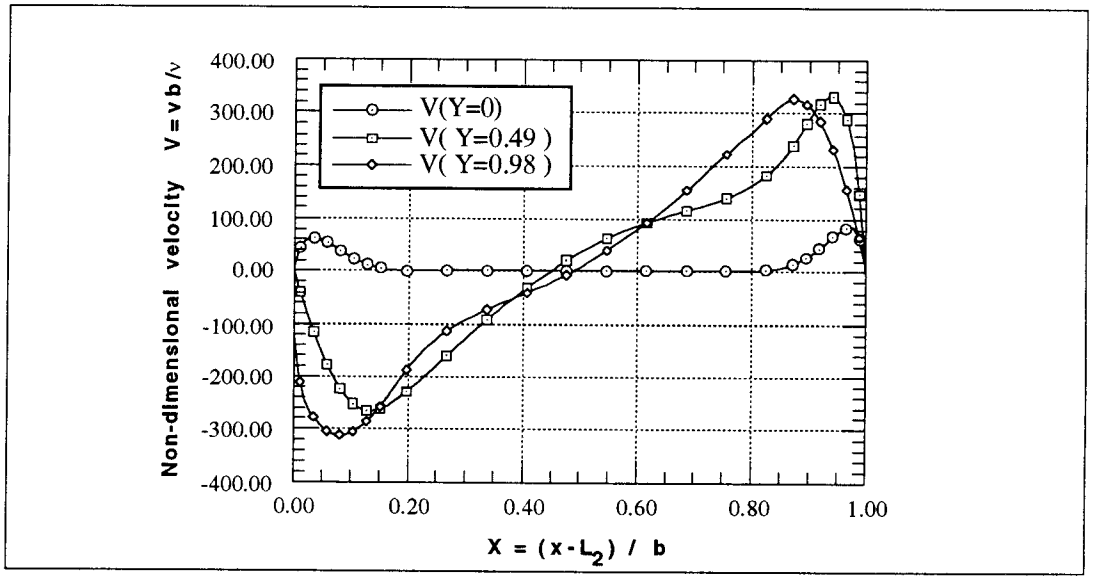

Figure 18: Non-dimensional velocity profile for $\Gamma = 3.6$

Figures 19 and 20 show regular boundary-layer-type velocity profiles along a vertical plate. When $\Gamma = 4.6$, the entrance profile shows a more vigorous flow next to plate A than next to plate B. The entrance velocity is zero as shown in Figure 19. For $\Gamma = 9.75$, Figure 20 shows the same trend, but there is a finite velocity at the entrance. This entrance velocity profile, although a little skewed to the left, is almost uniform. In both cases, at midheight, boundary layers have developed but not yet merged, and a very weak flow goes down in the middle. Analysis of the exit profile shows the presence of a reverse flow cell just above plate B. The flow coming up from the bottom along plate B bends toward plate A as a result of the formation of that circulation cell.

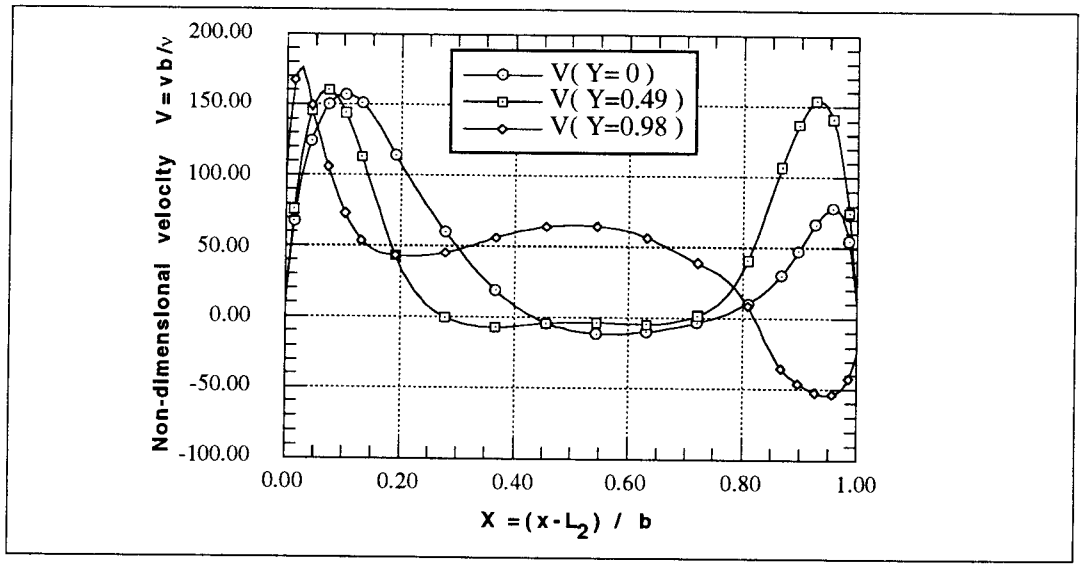

Figure 19: Non-dimensional velocity profile for $\Gamma = 4.6$

Figure 21 shows parabolic profiles at the entrance and mid-height. They are characteristics of fully-developed flow. Boundary layers from plates A and B have merged, and therefore, the effect of viscosity extends over the entire channel. At the exit, the parabolic profile is a little skewed to the left, indicating that the flow bends toward plate A. Here, however, no downward velocity appears, the circulation cell above plate B seems to have vanished.

One may ask why the two lower profiles don't start at zero at the wall. The reason is because a spline fit has been used rather than a regular linear fit to show the parabolic profile form. A linear fit would have passed through zero. This observation shows how poorly this grid spacing approximates the real profile. To study this area better, one should decrease the grid spacing by at least a factor of three.

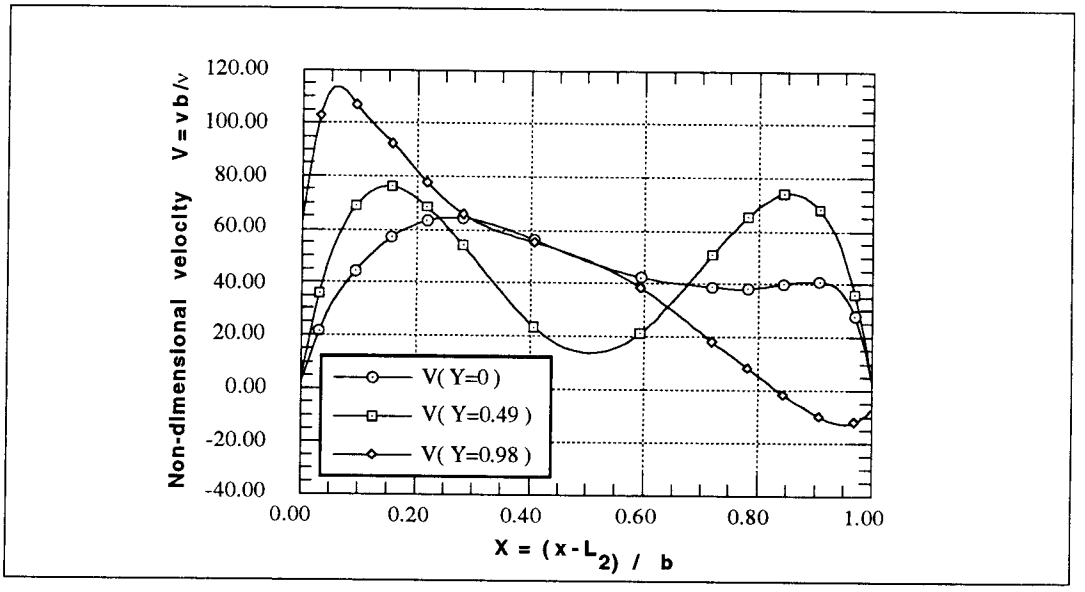

Figure 20: Non-dimensional velocity profile for $\Gamma = 9.75$

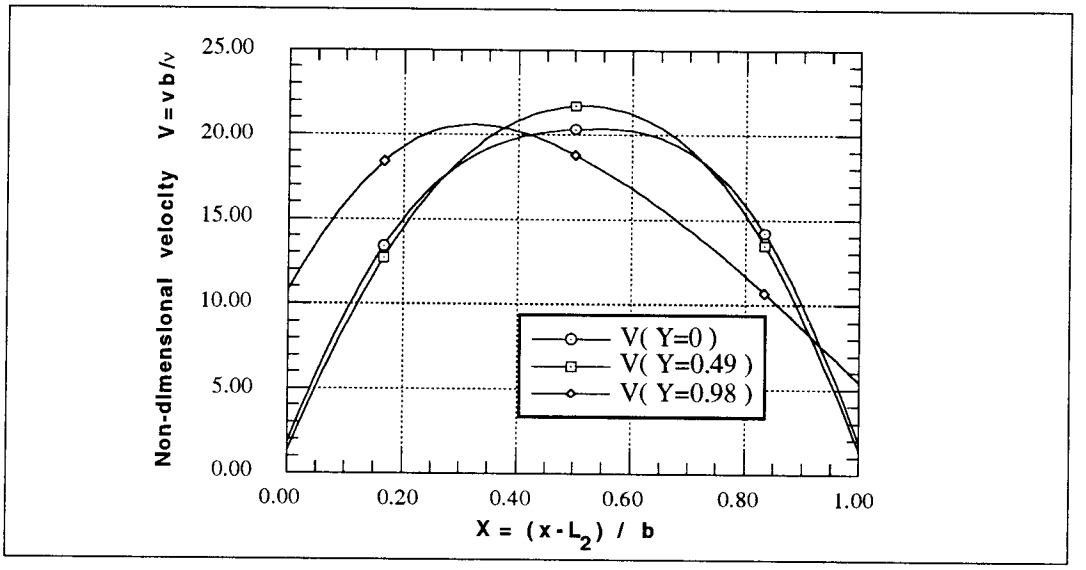

Figure 21: Non-dimensional velocity profile for $\Gamma = 52$

5.5 Streamlines and Isotherms

The output from simulation set number 3 ($q''' = 10^5$ W/m^3) was used to plot streamlines and isotherms for four configurations: Γ =3.6,4.6,9.75 and 52 as shown in Figures 21 and 22. In these streamline plots, dashed lines represent a clockwise flow while plain lines represent a counter-clockwise flow.

In Figure 21, one can observe the two limiting cases, 3.1 and 3.19, for which the flow shows the same characteristics as flow in a rectangular enclosure, featuring a large circulation cell whose center appears to be in the upper third of the enclosure. A smaller clockwise circulation cell appears just above plate B.

This cell grows to nearly fill the channel as plate A is moved away from the constant temperature wall. As it approaches plate B, the cell's size decreases but still forces the flow to go through a much smaller section than if there were no enclosure. This, of course forces the flow velocity to increase to maitain a fixed flow rate. One may wonder whether the cell is forming because the flow velocity is increased or whether the velocity increases because of the cell formation. The first choice seems more realistic but no clear answer can be given at this point.

Cool air rises along both faces of plate A in configurations 3.6 and 3.12, but in configuration 3.6, the flow hesitates in the middle of the channel before being pulled up along plate B. In configuration 3.12, a vigorous circulation cell has formed on the right face of plate A and the flow in the channel become more and more vigorous, becoming fully-developed.

Figure 22 shows isotherms for the same four configurations. These plots give us information about the constant heat flux assumptions and about the adequacy of grid spacing. In configuration 3.1,

obviously the constant flux configuration does not hold. The influence of the constant temperature wall is clear here showing the dominance of conduction effects relative to convection. In configurations 3.6 and 3.12, the constant flux assumption is confirmed. One can also observe that at the same altitude, plate B is hotter than plate A.

In configuration 3.19, the absence of grid points in the channel is apparent, the profile in plate A not being flat. Even though the heat fluxes on both faces of plate A are very different as shown by the difference in slopes of the isotherms, they remain approximately constant and thus the constant heat flux assumption still holds.

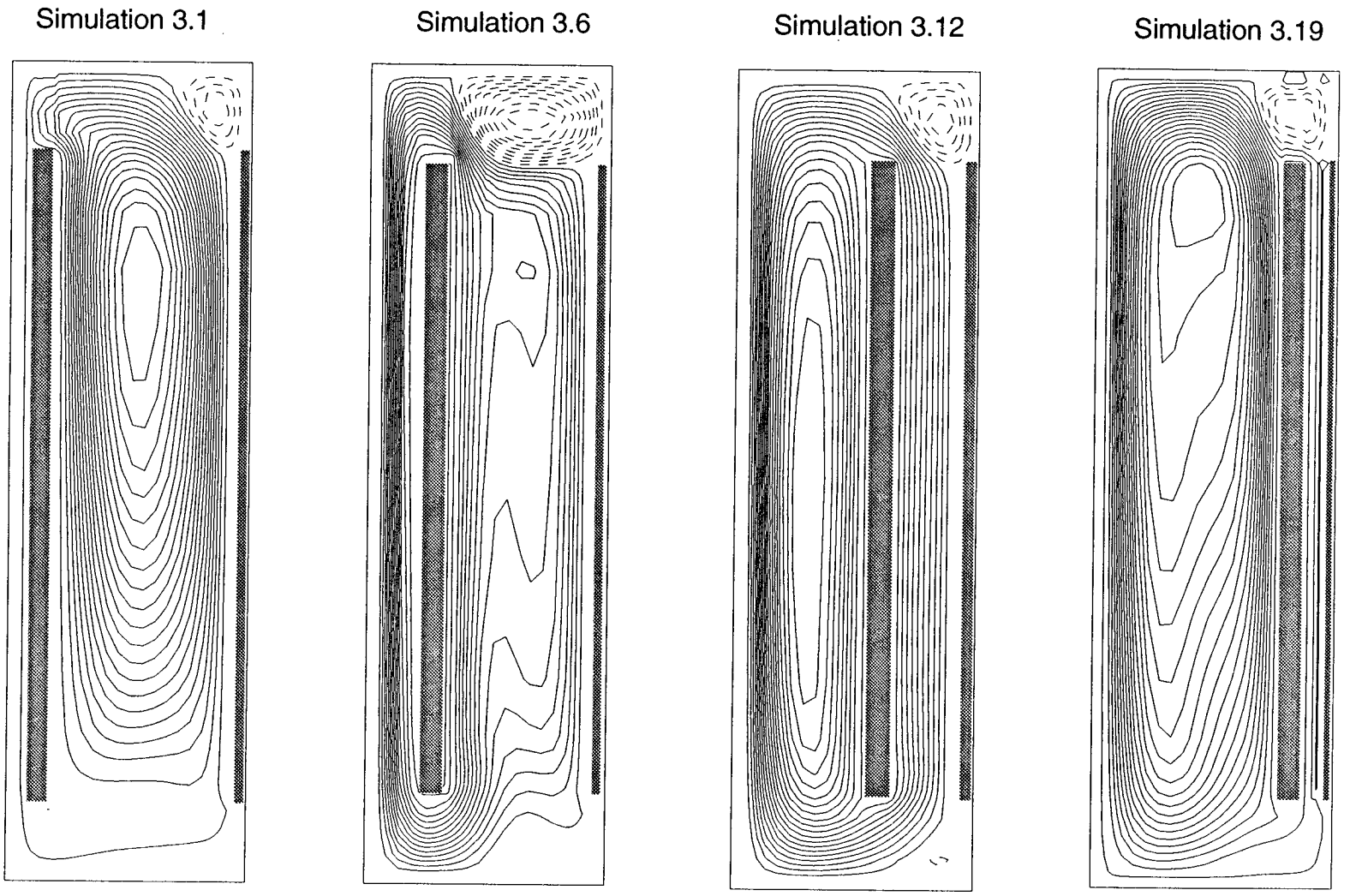

Figure 22: Streamline plot for the simulations 3.1, 3.6 ,3.12 and 3.19 — the channel aspect ratio is respectively 3.6, 4.6, 9.75 and 52

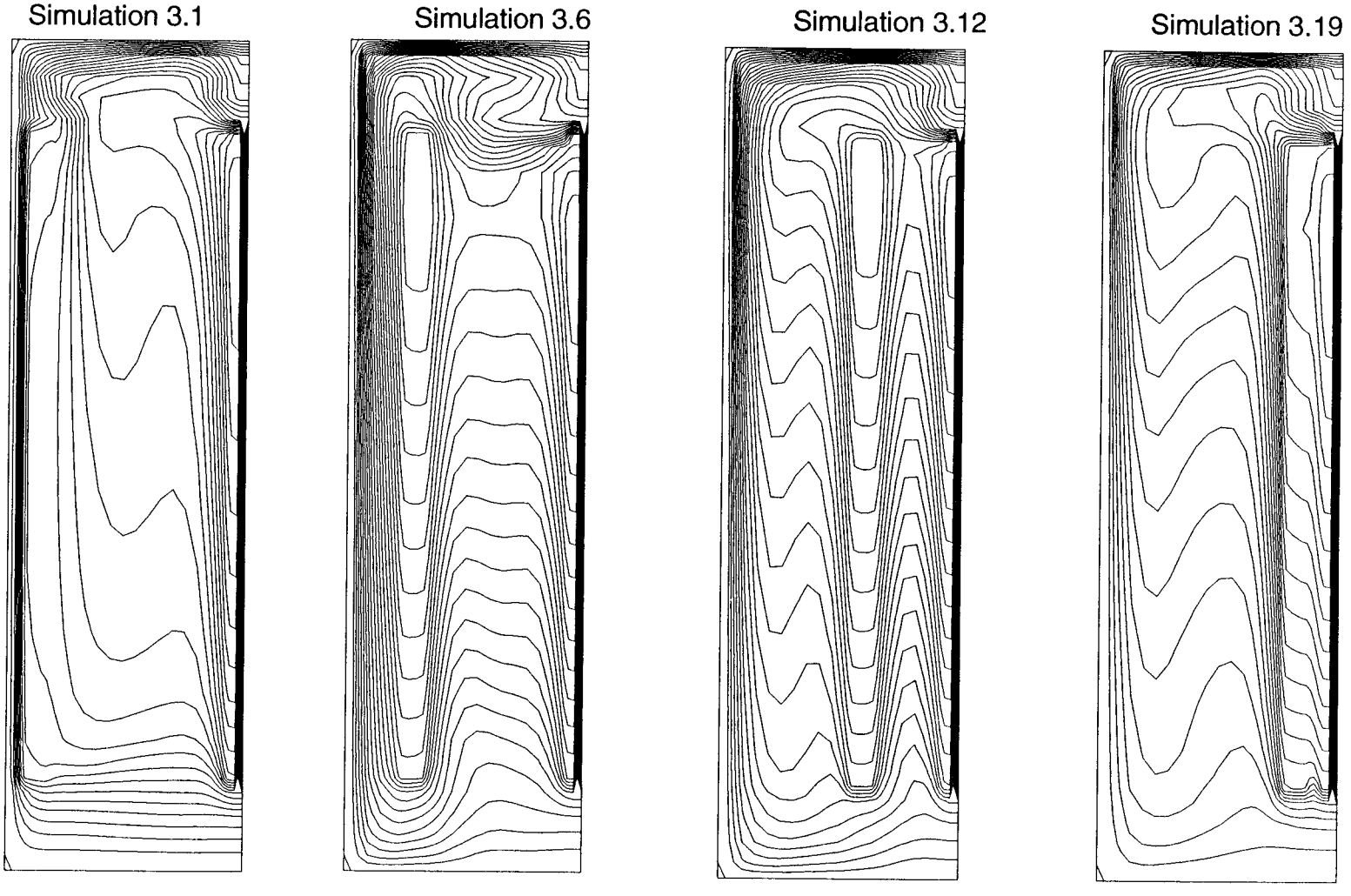

Figure 23: Isotherms for the simulations 3.1, 3.6, 3.12 and 3.19 — the channel aspect ratio is respectively 3.6, 4.6, 9.75 and 52

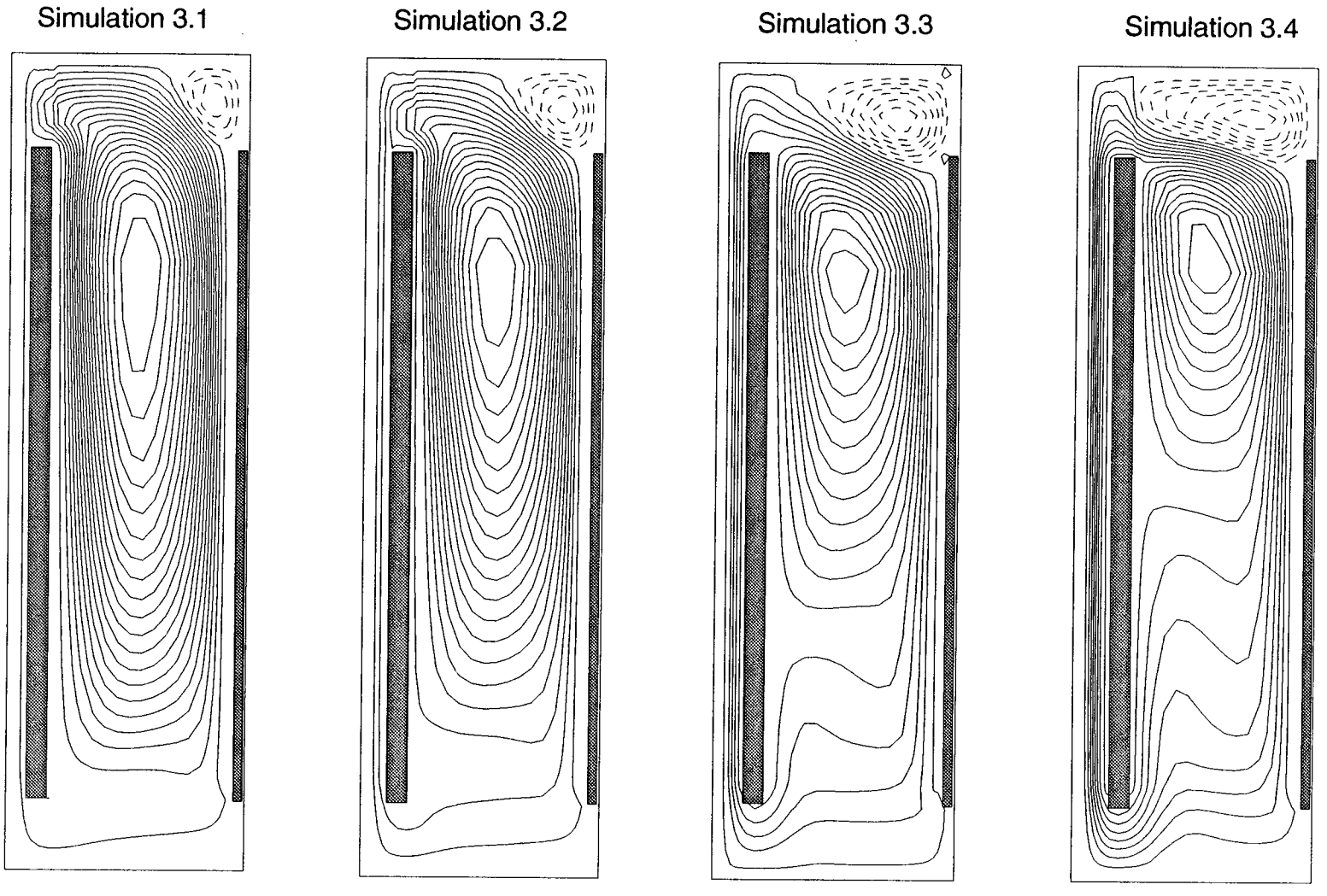

Figure 24: Effect of the constant temperature wall on the flow — Streamlines for small channel aspect ratios

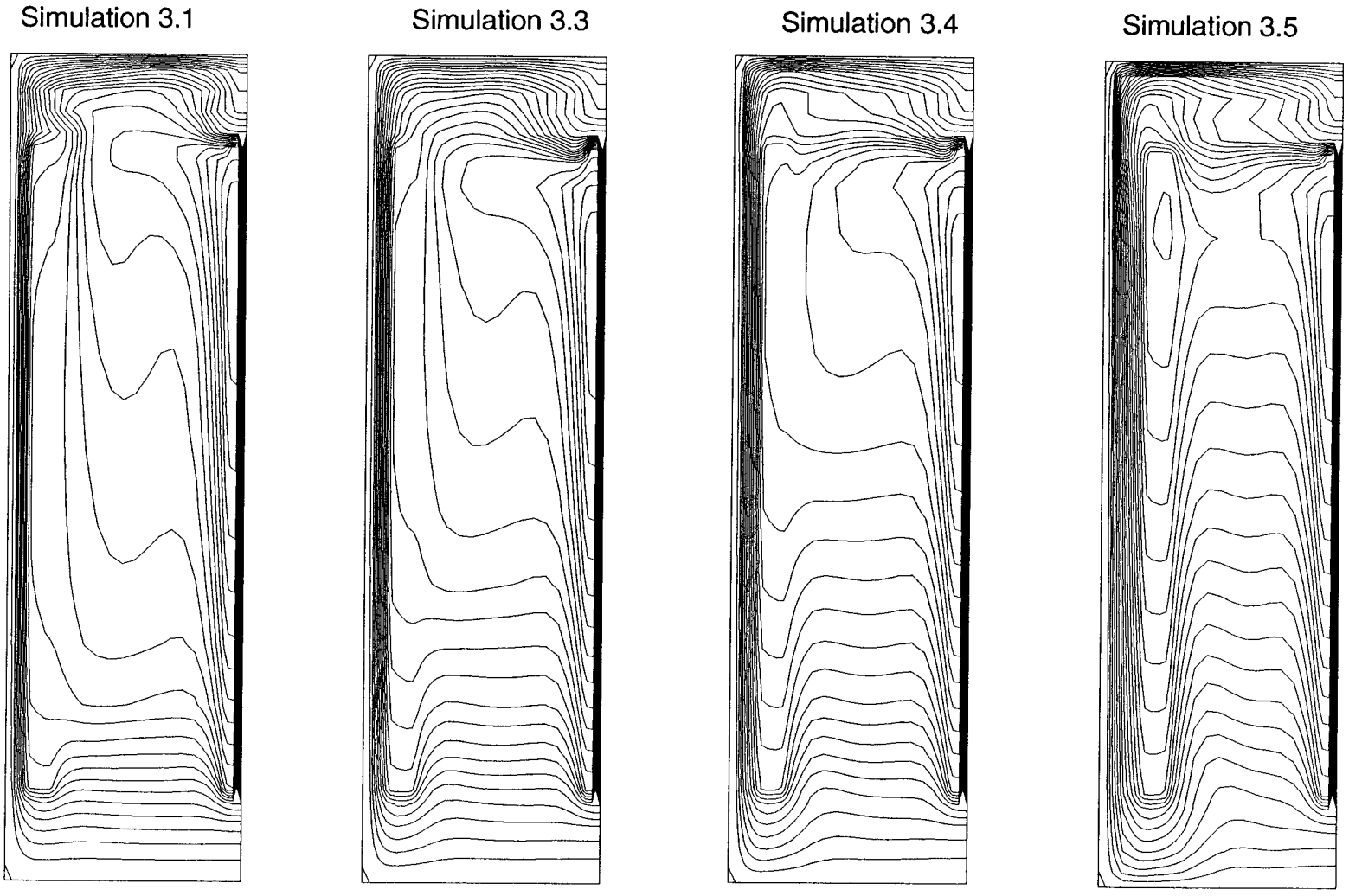

Figure 25: Effect of the constant temperature wall — Isotherms for small channel aspect ratio

5.6 Determination of the optimum channel width

The determination of an optimum value, b_{opt}, for each set of simulations can be accomplished in two steps by observing at Figures 26 and 27.

Figure 26 shows the maximum temperature in plate B, which is always higher than in plate A; it will therefore be the maximum tempera ture in the system. This plot shows that, even though we can find an absolute minimum for each set of simulations, it is probably more realistic to observe that the temperature reaches a low-temperature plateau. This plateau occurs for a range of Rayleigh numbers that produces constant and equal heat fluxes on all faces of the plates.

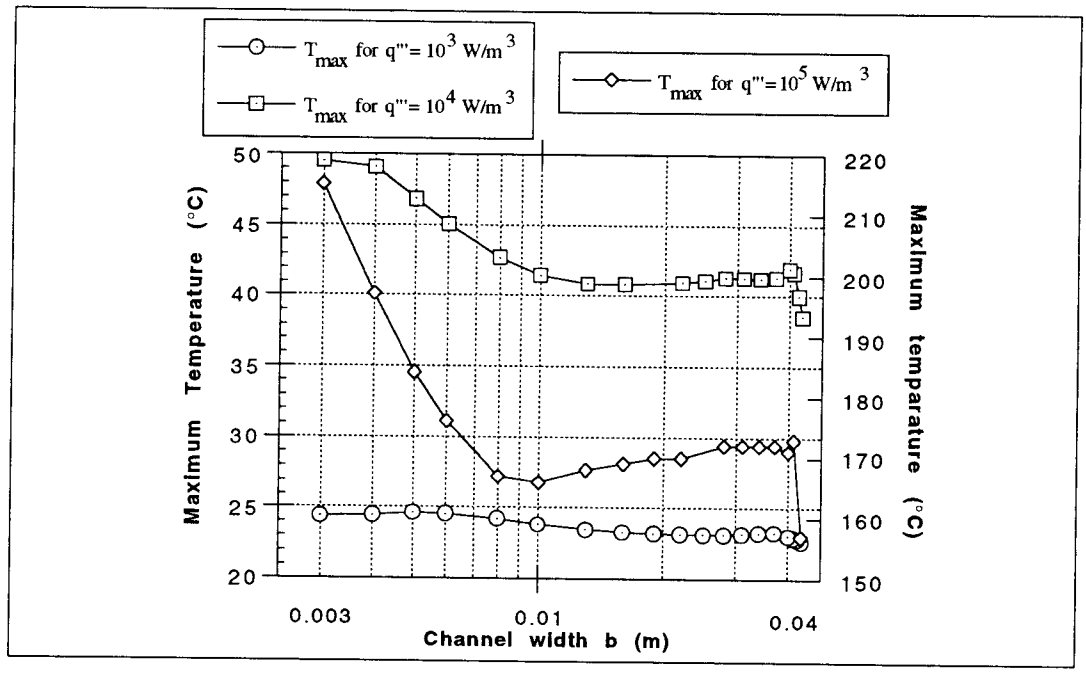

Figure 26: Maximum temperature on plate B as a function of channel width

A second step, according to paragraph 4.3.6, then consists in plotting NuL_3/b versus L_3/b, as shown in Figure 27, and trying to find a maximum. Figure 27 shows that, as q''' decreases, the optimum location for plate A varies over a smaller range. For $q''' = 10^3$ W/m^3, a specific optimum is found at $L_3/b = 7.5$; for the other two values of q''' used in these simulations, even though absolute maxima were achieved, it seems more reasonable to give a range for L_3/b — $L_3/b \in [5;17]$ for $q''' = 10^5$ W/m^3 and $L_3/b \in [5,15]$ for $q''' = 10^4$ W/m^3.

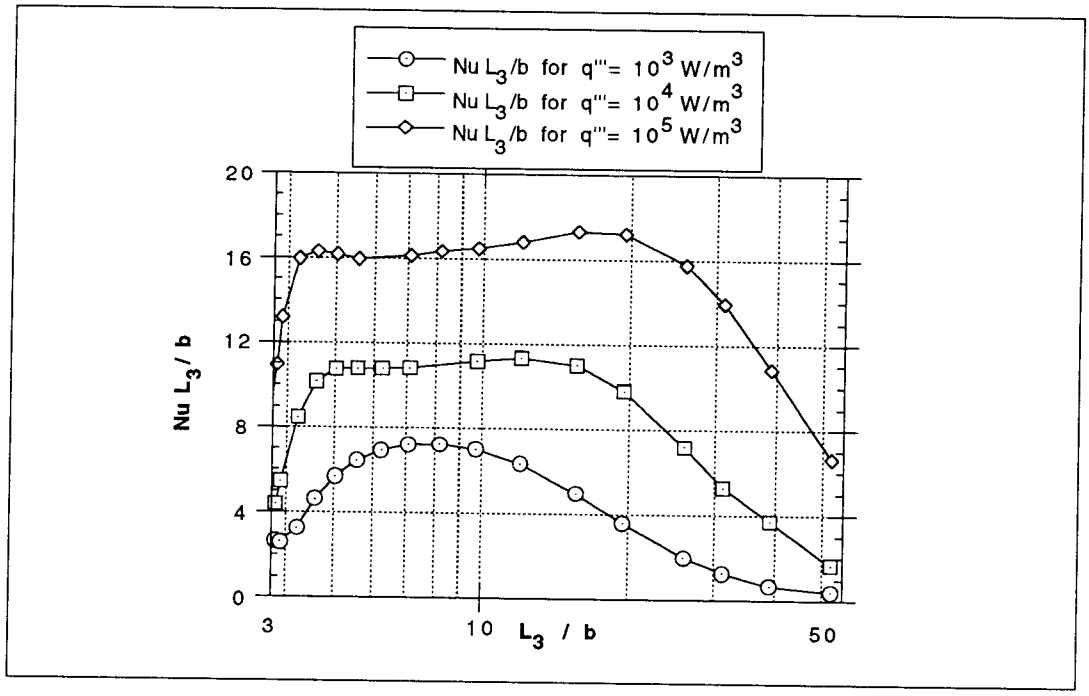

Figure 27: Plot of NuL_3/b as a function of the channel aspect ratio

CHAPTER VI: CONCLUSIONS

6.1 Conclusion

With the data obtained from the numerical simulation of the natural convection along 3 vertical plates in an enclosure, the following conclusions can be drawn.

A correlation for the average Nusselt number in the channel was obtained with a maximum error of 15.8 percent. The standard deviation error is less than 2.5 percent and the coefficient ,r^2=0.997.

$$Nu = \left((0.131Ra''^{0.5})^{-6} + (0.278\ Ra''^{0.2})^{-6}\right)^{-1/6}$$

where $Ra'' \in [0.1,\ 10^6]$

This result was obtained for these geometrical characteristics:

H= 20 cm L = 10 cm h= 15.6 cm

This correlation cannot be be considered absolutely correct since no experimental data are available to confirm it. However, it seems very reasonable since it is in very good agreement with the literature in the lower range of Ra" and has a similar behavior in the upper range.

Optimum values of the plate spacing, b_{opt}, were found for the three levels of heat generation studied:

- b_{opt} = 0.0208 m for $q''' = 10^3$ W/m^3
- b_{opt} = [0.009 , 0.03] for $q''' = 10^4$ W/m^3
- b_{opt} = [0.01, 0.03] for $q''' = 10^5$ W/m^3

For the higher values of q''', the determination of a unique optimum was difficult since temperature variation were small. The range given becomes wider as q''' increases. The range results also are an indication that the enclosure aspect ratio could be changed with the temperature remaining constant.

The maximum temperature obtained for the three optimum values were:

- $T_{max} = 23\ °C$ for $q''' = 10^3\ W/m^3$
- $T_{max} = 41\ °C$ for $q''' = 10^4\ W/m^3$
- $T_{max} = 165\ °C$ for $q''' = 10^5\ W/m^3$

The maximum temperature reached on plate B was near its top.

Conduction heat transfer becomes dominant relative to convection when plate A is close to the constant-temperature wall. This results in a dramatic drop for the average Nusselt number. In this case the system behaves very much like an enclosure with three constant temperature walls and one heated wall. The constant temperature wall boundary is an approximation; for a more realistic situation it should be replaced by a wall cooled by convection on its outside.

Streamlines for different locations of plate A show large flow pattern variations. In the configuration used, circulation cells were forming either in the channel or between the wall and plate A, as well as above the exit of the channel.

6.2 Recommendations

Due to limitations in time, this study has been very restricted. It could be expanded in a number of different ways, with a few modifications made to obtain useful results.

First of all, the boundary condition at the enclosure wall should be changed from one at constant temperature to a conductive wall with convection at the outside. This would reflect more accurately what is true in the real world. It would also be much easier to set up an experiment to confirm the numerical results.

Simulations should be run with various enclosure/plate height ratio, H/h to have an indication of the influence of the "nozzle" at the exit of the channel.

Simulations should be done by changing the enclosure ratio, H/L, to evaluate the influence of the enclosure geometry on the flow.

More simulations should be run over a wider range of q''' to define more accurately the relationship between b_{opt} and q'''.

Experiments should also be performed to try to confirm the numerical results.

BIBLIOGRAPHY

[1] Elenbaas, W., 1942, "*Heat Dissipation of Parallel Plates by Free Convection*," PHYSICA, Vol. 9, pp 1-28.

[2] Aung, W., Fletcher, L. S., and Sernas, V. 1972, "*Developing Laminar Free Convection Betyween Vertival Flat Plates With Assymetric Heating*," INTERNATIONAL JOURNAL OF HEAT AND MASS TRANSFER, Vol. 15, pp. 2293-2308.

[3] Jonhson, C.E., 1986, "*Evaluation of Correlations for Natural Convection Cooling of Electronic Equipment*," HEAT TRANSFER ENGINEERING, Vol. 7 Nos. 1-2, pp. 36-45

[4] Wirtz and Stutzman, R.A., and Stutzman, R.J., 1982, "*Experiments on Free Convection Between Vertical Plates With Symmetric Heating*," ASME JOURNAL OF HEAT TRANSFER, Vol. 104, pp. 501-507.

[5] Bar-Cohen, A., and Rohsenow, W.M., 1984, "*Thermally Optimum Spacing of Vertical Natural Convection Cooled, Parallel Plates*," ASME JOURNAL OF HEAT TRANSFER, Vol. 106, pp.116-123.

[6] Birnbrier, H., 1981, "*Experimental Investigations on the Temperature Rise of Printed Circuit Boards in Open Cabinets With Natural Ventilation*," HEAT TRANSFER IN ELECTRONIC EQUIPMENT, M.D. Kelleher and and M.M. Yovanovich, eds., ASME HTD - Vol. 20, pp.19-23.

[7] Kim,S.H., Anand,N.K., and Fletcher,L.S., 1989, "*Free Convection Between Series of Vertical Parallel Plates With Embedded Line Heat Sources*," NUMERICAL SIMULATION OF CONVECTION IN ELECTRONIC EQUIPMENT - ASME HTD- Vol 121, pp.7-16.

[8] Ramanathan,S., and Kumar, R., 1991, "*Correlation for Natural*

Convection Betwenn Heated Vertical Plates," TRANSACTION OF THE ASME, JOURNAL OF HEAT TRANSFER, Vol. 113, pp97-107.

[9] Trent, D.S., and Eyler,L.L., 1991, "*TEMPEST A Computer Program for Three-Dimensional Time-Dependent Hydrothermal Analysis*," BATTELLE PACIFIC NORTHWEST LABORATORIES.

[10] Feldman, S.I., Gay, D.M., Maimone, M.W., and Schryer, N.L., 1990, "*A Fortran-toC Converter*," COMPUTER SCIENCE TECHNICAL REPORT NO. 149, AT&T Bell Laboratories.

[11] Pulliam, T.H., 1990, "*NXcontour V1.0*," NASA AMES RESEARCH CENTER.

[12] Kaleidagraph™ Version 2.1.3, 1991"*Data Analysis and Graphic Presentation for Business, Science and Engineering*," ABELBECK SOFTWARE.

[13] Churchill, S.W., and Usagi, R. 1972, "*A General Expression for the Correlation of Rates of Heat Transfer and Other Phenomena*," JOURNAL OF AMERCAN INSTITUTE OF CHEMICAL ENGINEERS, Vol.18, pp 1121-1138.

Appendices

Appendix A

Input file for TEMPEST

```
* 3.6- variable grid - with symetry- q= 1e4 w/m3 - test input every 5sec
size,   34   24    1
time,   .1       100
prnt,   60                                   100
pres,   50       1.1  1-9
post,  100
```

} Group No. 1

```
cont,heat,pace,sisy,dtim,psav,form,
dbug,prop,size,data,ntyp,init,
aout,velz,velr,temp,
plot,velr,velz,temp,
```

} Group No. 2

```
  0    2                1   34    1   24    1    1                        1
 60    3    1           1    1    1   24    1    1                        1
 60    3    1           1   34    1    1    1    1                        1
 60    3    1           1   34   24   24    1    1                        1
 20    3    1          34   34    1   24    1    1                        1
 70    1    1          10   13    6   19    1    1                        1
 70    1    1          32   33    6   19    1    1                        1
                        9    9    6   19    1    1          1    1    3
                       13   13    6   19    1    1          1    2    3
                       31   31    6   19    1    1          1    3    3
```

} Group No. 3

```
              1                        90  180   90                        1cm
.25   .1    .1   .1   .3   .3   .1   .1   .1   .1    1   10              3cm
 .2   .2    .1   .1   .1   .1   .1   .1   .3   .3   11   20              3cm
 .3   .3    .3   .3   .3   .3   .1   .1   .1   .1   21   30              3cm
 .1   .1    .2   .2                                 31   34              3cm
.25   .5    .5   .5   .5   .2   .4   .8  1.4  1.5    1   10              4cm
1.5   2.    2.  1.5  1.5  1.4   .8   .4   .2   .5   11   20              4cm
 .5   .5    .5  .25                                 21   24              4cm
                                 20  -20  900   61         11    2cg   6si
 .5   20 380.                    20                    0    1cs   6si
1+3239.3 380.                    20                    0    3cs   6si
 20  1+4                             10   13    6   19                   9si
 20  1+4                             32   33    6   19                   9si
 20                                   1   34    1   24                   9si
  0   1.                                                      1    16si
180   1.                                                      1    16si
  0   1.  180   1.                                       2    1    24si
```

} Group No. 4

The input file for TEMPEST is made of four blocks of data called group. Group No. 1 provide TEMPEST with the initialization and numerical control parameter. Group No.2 provide the alphanumeric control parameters. Group No. 3 the integer data and group No.4 the floating-point data.

The input file shown in the previous pagecan be read as follow:

• Group No.1

- there are 34 cells in the x-direction and 24 in the y-direction
- the starting time step is .1 second and the simulation time is 100 seconds
- a print out is asked at t= 100 seconds
- the maximum pressure iteration is 50, the acceleration factor 1.1 and the pressure error allowable 10^{-9}
- a postprocessing file should be created at t= 100 seconds

• Group No.2

- TEMPEST should solve the energy equation using the international units system and by choosing the most efficient time step.
- TEMPEST should create an ouput including the cells type and different other thing for debuging purpose.
- the velocities and temperature should be recorded in both the postprocessing file and the output file.

• Group No.3

- Cells are given different types: 0, computational cell; 60, constant tempearture cells, and 70, heat generation cells.
- Surfaces to compute the flux over is pecified.

• Group No.4

- Grid spacing is specified for both direction
- Material properties are specified.
- Time specification for initial conditions and boundary conditions are specified.

Appendix B

Computational Grid

Symmetry cells

Heat generation cells

Constant temperature cells

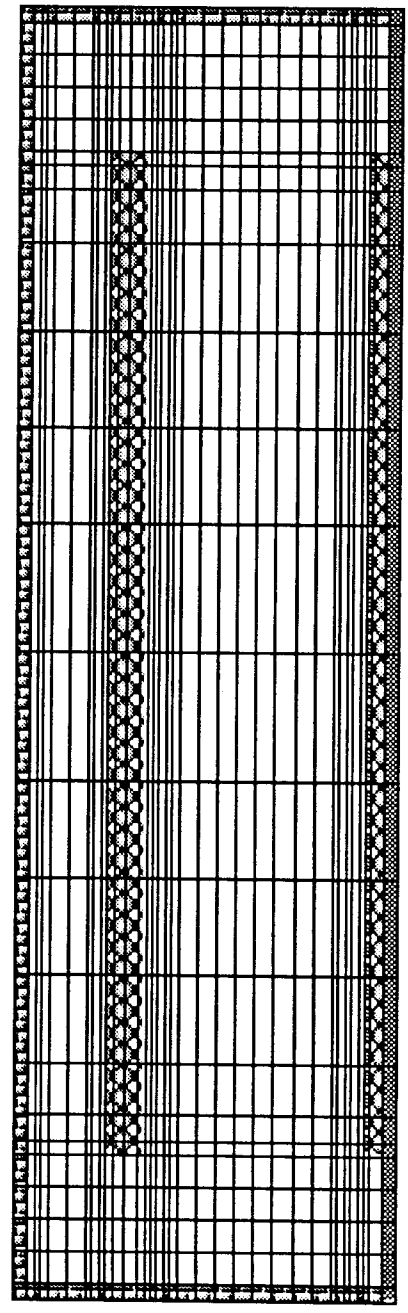

Appendix C

Postprocessing Fortran subroutine

```
c**-----------------------------------------------------------------
--
c**   special routine set so user can do what he wants to the
TEMPEST
c**   data u,v,and t read with READER, a program to convert
TEMPEST
c**   binary files into ASCII files.
c**-----------------------------------------------------------------
--

      subroutine usersub(nr,nz,nar,uu,vv,tt)
      implicit none

      integer mxgrid,mxinpt

      parameter (mxgrid=100)
      parameter (mxinpt=60)
```

```
      save

c**-----------------------------------------------------------------
--
c**   declaration of variables
c**-----------------------------------------------------------------
--
      character*5 test
      character*80 title
      character*12 infile,nufile,dcpiso,dcpstr
      character*12 dumb,grids,gridt
      integer card, id,i,j,k,firstr,firstz,nr10,nz10,nplate
      integer lower,upper,loca,first,norm,nz,nr,middle,nar
      real*8 input,psi,vel,uu,vv,tt
      real*8 dr,dz,r,z,rphi,zphi
      real*8 q,qtheo,a,b,l,H,Pr,w,Gbeta,Tref,km,rho,cp,mu,nu,ka
      real*8
L1,L2,X,Y,U,V,T,rh,rt,NuB,RaB,Tmax,Nulow,Numin,Nu2, Nu3, Nu1
      logical varr, varz
      dimension norm(10),q(0:3)
      dimension input(mxinpt,13),id(mxinpt)
      dimension r(mxgrid),z(mxgrid), dr(mxgrid),dz(mxgrid)
      dimension rphi(mxgrid),zphi(mxgrid)
      dimension psi(mxgrid,mxgrid),vel(mxgrid,mxgrid)
      dimension loca(6), T(mxgrid,mxgrid),Tmax(mxgrid)
```

```
      dimension
X(mxgrid),Y(mxgrid),U(mxgrid,mxgrid),V(mxgrid,mxgrid)
      dimension uu(nar,nar),vv(nar,nar),tt(nar,nar)

c**-----------------------------------------------------------------
--
c**   initialize variable
c**-----------------------------------------------------------------
--
      card=1
      do 10 j=1,40
         id(j)=0
10    continue

      do 20 k=1,13
      do 20 j=1,40
         input(j,k)=0
20    continue
      varr=.false.
      varz=.false.


      print *,'Which input file do you want to open ?'
      read (*,900) infile
      i=1
```

```
 30   if(infile(i:i).eq.' ') then
         goto 40
      else
         i=i+1
         goto 30
      endif
 40   continue
      i=i-1
      title= infile(1:i)
      nufile="nusselt"
      gridt=infile(1:i)//'.gt'
      grids=infile(1:i)//'.gs'
      dcpiso=infile(1:i)//'.dt'
      dcpstr=infile(1:i)//'.ds'

      open(unit=10, file=infile(1:i))
      open(unit=11,file=nufile,status='old')
c     open(unit=12,file=grids)
c     open(unit=14,file=gridt)
c     open(unit=15,file=dcpiso)
c     open(unit=16,file=dcpstr)
      open(unit=17,file="cvgce",status='old')

c**-----------------------------------------------------------------
--
```

```
c** read the input file to get grid and material properties.
c**-----------------------------------------------------------------
--
c** If id(i)=1,3,4 or 5 this line of input is a line that
gives us
c** the grid spacing (uniform if id=1, non uniform in r-
direction
c** if id=3, in z-direction if id=4, in x direction if id=5.
c** If id=6 then we are dealing with a material property
input line.
c**     We read,   kk - thermal conductivity
c**          rho - density
c**          cp - specific heat
c**          mu - dynamic viscosity
c**          co - brine concentration
c**          po - ref pressure
c**          to - ref temperature
c**     Then we read the material number in field 13 and id
in field 14
c**
c**-----------------------------------------------------------------
--
    i=0
50  read(10,900) test
    if (test.eq.'          ') then
```

```
        card=card+1
c**-------------------------------------------------------------
--
c**     card #3 is the one  giving the plate position
c**-------------------------------------------------------------
--
       if (card.eq.3) then
60         i=i+1
           read(10,905) (input(i,j),j=1,13),dumb
           id(i)=ichar(dumb(5:5))-48
           if((id(i).eq.1).or.(id(i).eq.3)) then
              goto 60
           endif
           card=card+1
       endif

c**-------------------------------------------------------------
--
c**     card type 4 give the spacing and material properties
c**-------------------------------------------------------------
--
       if (card.eq.4) then70
          i=i+1
          read(10,905, end=80) (input(i,j),j=1,13),dumb
          id(i)=ichar(dumb(5:5))-48
```

```
if((ichar(dumb(4:4)).ge.48).and.(ichar(dumb(4:4)).le.57))
then
            id(i)=id(i)+10*(ichar(dumb(4:4))-48)
            if(id(i).eq.-16) then
                goto 80
            endif
            endif
            goto 70
        endif
    endif
    go to 50
80  continue


c**-------------------------------------------------------------------
--
c** compute grid  and initialize materials
c**-------------------------------------------------------------------
--
c** Check if non uniform grid in either r or z direction
c**-------------------------------------------------------------------
--
    print *, id(j), j
    first =j   do 90 j=i-3 ,1,-1
```

```
        print*,   id(j),j
        if(id(j).eq.-16) then
           goto 100
        endif

        if (id(j).eq.3) then
           varr=.true.
           firstr=j
        endif
        if (id(j).eq.4) then
           varz=.true.
           firstz=j
        endif
        if( id(j).eq.1) then
           first=j
        endif90    continue
100 continue
c**-------------------------------------------------------------
--
c**     Create r-direction grid
c**-------------------------------------------------------------
--  print *, varr,varz, firstz,firstr
    if (varr) then
      nr10=nr/10
      do 110 i=1,nr10
```

```
        do 120 j=1,10
            dr(j+(i-1)*10)=input(firstr,j)*1e-2
120     continue
        firstr=firstr+1
110   continue
      do 130 j=1,nr-10*nr10
        dr(10*nr10+j)=input(firstr,j)*1e-2
130   continue
    else
      do 140 i=1,nr
        dr(i)=input(first,1)*1e-2
140   continue
    endif

    r(1)=-dr(1)/2.0
    do 150 i=2,nr
       r(i)=r(i-1)+dr(i)/2.0+dr(i-1)/2.0
150 continue
c**-----------------------------------------------------------------
--
c** Create z-direction grid
c**-----------------------------------------------------------------
--

    if (varz) then
```

```
      nz10=nz/10
      do 170 i=1,nz10
       do 160 j=1,10
          dz(j+(i-1)*10)=input(firstz,j)*1e-2
160    continue
       firstz=firstz+1
170   continue
      do 180 j=1,nz-10*nz10
       dz(10*nz10+j)=input(firstz,j)*1e-2
180   continue
    else
      do 190 j=1,nz
          dz(j)=input(first,2)*1e-2
190   continue
    endif

    z(1)=-dz(1)/2.0
    do 200 i=2,nz
       z(i)=z(i-1)+dz(i)/2.0+dz(i-1)/2.0
200 continue

c**-----------------------------------------------------------------
--
c** Physical properties initialization
c**-----------------------------------------------------------------
```

```
--

      Tref=20
      Pr= 0.72
      ka=0.0248
      Gbeta = 107/.72*1e6
      nu= 0.15e-4
      i=1
      nplate=0
      j=0
c**-----------------------------------------------------------------
--
c**         Read plate location
c**
c** % loca gives the r-direction cell # of a face of a plate
c** % norm gives the normal orientation of the face
c**
c**-----------------------------------------------------------------
--

210 if (input(i,1).eq.70) then
        nplate =nplate+1
        print *,'nplate',nplate
        j=j+2
        loca(j-1)=input(i,5)
```

```
          norm(j-1)=-1
          loca(j)=input(i,6)
          norm(j)=+1
          upper= input(i,8)
          lower= input(i,7)
          middle= (upper-lower)/2
 + lower    print *,loca(j-1),loca(j),upper,lower, middle
          if(input(i+1,1).ne.70) then
             goto 220
          endif
      endif
      i=i+1
      goto 210
c**-------------------------------------------------------------------
--
c**         Read other data
c**-------------------------------------------------------------------
--

220     continue
     if ((id(i).eq.6).and.(input(i,13).eq.1)) then
         km=input(i,1)
         rho=input(i,2)
         cp=input(i,3)
         mu=input(i,4)
```

```
      print *,'km=',km,'  rho=',rho,'  cp=',cp
      goto 230
    endif
    i=i+1
    goto 220
230 continue


c**-----------------------------------------------------------------
--
c**        Compute l, b, H, a, w, L1, L2
c**-----------------------------------------------------------------
--
    print *, upper, lower,nz
    print *, z(lower), z(upper), dz(upper)
    l= z(upper)-z(lower)+dz(lower)/2.0+dz(upper)/2.0
    H= z(nz)-(dz(1)+dz(nz))/2.0
    b= r(loca(3))-r(loca(2))-(dr(loca(2))+dr(loca(3)))/2.0
    a= r(loca(2))-r(loca(1))+(dr(loca(1))+dr(loca(2)))/2.0
    w= r(loca(1))-dr(1)-dr(loca(1))/2.0
    L1= z(lower)
    L2= r(loca(2))
    print * ,l,H,b,a,w
c**-----------------------------------------------------------------
--
```

```
c**        Compute surface flux.
c**-----------------------------------------------------------------
--

    qtheo= 1e5*a
    q(0)=0
    q(1)=0
    q(2)=0
    q(3)=0
    do 240 j=lower,upper
       q(0)= q(0)-2*(tt(1,j)-tt(2,j))/
     &  (dr(2)/ka+dr(1)/km)/l*dz(j)
       q(1)= q(1)-2*(tt(loca(1)-1,j)-tt(loca(1),j))/
     &  (dr(loca(1)-1)/ka+dr(loca(1))/km)/l*dz(j)
       q(2)= q(2)-2*(tt(loca(2)+1,j)-tt(loca(2),j))/
     &  (dr(loca(2)+1)/ka+dr(loca(2))/km)/l*dz(j)
       q(3)= q(3)-2*(tt(loca(3)-1,j)-tt(loca(3),j))/
     &  (dr(loca(3)-1)/ka+dr(loca(3))/km)/l*dz(j)


240 continue
    print * ,'qtheo= ',qtheo
    print *, q(0)
    print *, q(1)
    print *, q(2)
```

```
      print *, q(3)
      print *, ''
c**-----------------------------------------------------------------
--
c** Non dimensionalize u, v and t
c**-----------------------------------------------------------------
--

      do 500 i= 1, nr
         X(i) = (r(i)-L2)/b
500   continue
      do 510 j=1,nz
         Y(j) = (z(j)-L1)/b
510   continue
      do 520 j=1,nz
      do 520 i=1,nr
         U(i,j) = uu(i,j)*b/nu
         V(i,j) = vv(i,j)*b/nu
520   continue

c**-----------------------------------------------------------------
--
c** We compute the non dimensional Temperature T in the
channel B
c**-----------------------------------------------------------------
```

```
--
        do 530 j=lower, upper
     do 530 i=loca(2),loca(3)
        T(i,j) = (tt(i,j)-Tref)/(q(3)*b)*ka
530  continue

     Tmax(1)=0
     Tmax(2)=0
     Tmax(3)=0
     do 540 j=lower,upper
     do 540 i=1,3  if(tt(loca(i),j).ge.Tmax(i))then
           Tmax(i)=tt(loca(i),j)
     endif
540     continue

c**-------------------------------------------------------------
--
c**     Initialize U for stream functions
c**-------------------------------------------------------------
--
     do 250 j=1,nz
     do 250 i=1,nr
        vel(i,j)=0
250  continue
```

```
      do 260 j=2,nz-1
      do 260 i=2,nr-1
         vel(i,j) =uu(i,j)
 260  continue

 c**-----------------------------------------------------------------
 --
 c**     compute stream functions with U
 c**-----------------------------------------------------------------
 --

     do 270 i=1,nr+1
        do 270 j=1,nz+1
           psi(i,j)=0
 270  continue
     do 280 j=2,nz
        do 280 i=2,nr
           psi(i,j)=psi(i,j-1)+dz(j-1)*vel(i-1,j-1)
 280     continue


 c**-----------------------------------------------------------------
 --
 c**     Compute grid for stream functions
 c**-----------------------------------------------------------------
```

```
--
      rphi(1)=r(1)-dr(1)/2.0
      do 290 i=1,nr
         rphi(i+1)=rphi(i)+dr(i)
290   continue

      zphi(1)=z(1)-dz(1)/2.0
      do 300 i=1,nz
         zphi(i+1)=zphi(i)+dz(i)
300      continue

c**-----------------------------------------------------------------
--
c**-----------------------------------------------------------------
--
c**     Compute Nusselt number
c**-----------------------------------------------------------------
--
c**-----------------------------------------------------------------
--
c**-----------------------------------------------------------------
--
      rh=q(2)/q(3)
      rt=(T(loca(2),middle)-Tref)/(T(loca(3),middle)-Tref)
      Nulow=1/T(loca(3),lower)*(1+rh)/(1+rt)
```

```
      NuB=1/T(loca(3),middle)*(1+rh)/(1+rt)
      Nu1= (L2-a)*q(1)/ka/(tt(loca(1),middle)-Tref)
      Nu2=b*q(2)/(tt(loca(2),middle)-Tref)/ka
      Nu3=b*q(3)/(tt(loca(3),middle)-Tref)/ka
      RaB=Gbeta*q(3)*b**5/l/ka*(1+rh)/2.0*Pr
c**-----------------------------------------------------------------
--
c**-----------------------------------------------------------------
--
c**     Create grid file for  NXcontour
c**-----------------------------------------------------------------
--
c**-----------------------------------------------------------------
--
c**     Temperature grid
c**-----------------------------------------------------------------
--
     open (unit=18,file= "grid.nx")
     do 320 j=1,nz
        do 320 i=1,nr
           write(14,925) r(i)
           write(18,925) r(i)
320  continue
     do 330 j=1,nz
        do 330 i=1,nr
```

```
            write(14,925) z(j)
            write(18,925) z(j)
 330 continue
     close(unit=18)

 c**-----------------------------------------------------------------
 --
 c**     Create Stream function grid file
 c**-----------------------------------------------------------------
 --
     open(unit=18,file="gridstr")
     do 340 j=1,nz+1
        do 340 i=1,nr+1
            write(12,925) rphi(i)
            write(18,925) rphi(i)
 340 continue
     do 350 j=1,nz+1
        do 350 i=1,nr+1
            write(12,925) zphi(j)
            write(18,925) zphi(j)
 350 continue
     close(unit=18)
 c**-----------------------------------------------------------------
 --
 c**     Create output file for isotherme and NXcontour
```

```
c**--------------------------------------------------------------
--
      open(unit=18, file= 'iso.nx')
      write(15,920) nr
      write(15,920) nz
      write(18,920) nr
      write(18,920) nz
      do 360 j=1,nz
         do 360 i=1,nr
            write(15,925) tt(i,j)
            write(18,925) tt(i,j)
360   continue
      close(unit=18)

c**--------------------------------------------------------------
--
c**     Create output file for U-Streamfunctions and
DCPcontour
c**--------------------------------------------------------------
--
      open(unit=18,file='stream.n')
      write (16,920) nr+1
      write (16,920) nz+1
      write (18,920) nr+1
      write (18,920) nz+1
```

```
      do 370 j=1,nz+1
         do 370 i=1,nr+1
            write (16,925) psi(i,j)*1e5
            write (18,925) psi(i,j)*1e5
370      continue
      close(unit=18)

c**-----------------------------------------------------------------
--
c**     Create output file for testing the convergence time
c**-----------------------------------------------------------------
--
380   read (17,900,end=390) dumb
      goto 380
390      continue
      backspace 17
      write(17,910) tt(lower-1,loca(1)),tt(upper+1,loca(1)),
     &  tt((upper+lower)/2,loca(3)),uu(lower-
1,loca(1)),uu(upper+1,
     &  loca(1)),uu((upper+lower)/2,loca(3)),vv(lower-
1,loca(1)),
     &  vv(upper+1,loca(1)),vv((upper+lower)/2,loca(3))
        write (17,900) ' '

c**-----------------------------------------------------------------
```

```
--
c**     Create output file for Nusselt number and run
characteristics
c**-------------------------------------------------------------------
--


400 read (11,900,end=410) dumb
    goto 400
410     continue
    backspace 11
    write(11,952)
title,RaB,NuB,Nulow,Nu1,Nu2,Nu3,Tmax(1),Tmax(2),      &
    Tmax(3),1/b,qtheo,q(0),q(1),q(2),q(3)

    open(unit=13, file='TX(Y)', status='old')
600 read (11,900,end=610) dumb
    goto 600
610     continue
    backspace 13
    do 620 i=loca(2), loca(3)
       write (13,950) T(i,lower),T(i,middle),T(i,upper),1/b
     & ,X(i),Y(lower)*b/1,Y(middle)*b/1, Y(upper)*b/1
620 continue
    close (unit=13)
```

```
      open(unit=13, file='TY123', status='old')
  630 read (11,900,end=640) dumb
      goto 630
  640     continue
      backspace 13
      do 650 j=lower,upper
         write(13,950)
 T(loca(2),j),T(loca(3),j),Y(j)*b/l,l/b,X(1),X(2),X(3)
  650 continue
      close (unit=13)

      open(unit=13, file='V(X)', status='old')
  660 read (11,900,end=670) dumb
      goto 660
  670     continue
      backspace 13
      do 680 i=loca(2), loca(3)
         write (13,950)
 V(i,lower),V(i,middle),V(i,upper),X(i),l/b
     &  ,Y(lower)*b/l,Y(middle)*b/l, Y(upper)*b/l
  680 continue
      close (unit=13)
      close(unit=10)
      close(unit=11)
```